

Ivan Nazarenko,
Leonid Pelevin,
Oleksandr Kostenyuk,
Oleg Dedov,
Anatoly Fomin,
Mykola Ruchynskyi,
Anatoly Sviderskyi,
Yevhen Mishchuk,
Volodymyr Slipetskyi

Applied problems of motion of mechanical systems under action of power loads

Monograph

Edited by
Doctor of Technical Sciences, Professor
Ivan Nazarenko

August, 2019

Published in 2019

by «Scientific Route» OÜ

Narva mnt 7-634, Tallin, Harju maakond, Estonia, 10117

© I. Nazarenko, L. Pelevin, O. Kostenyuk, O. Dedov, A. Fomin, M. Ruchynskiy, A. Sviderskiy, Ye. Mishchuk, V. Slipetskiy. 2019

All rights reserved. No part of this book may be reprinted or reproduced or utilised in any form or by any electronic, mechanical, or other means, now known or hereafter invented, including photocopying and recording, or in any information storage or retrieval system, without permission in writing from the authors.

This book contains information obtained from authentic and highly regarded sources. Reasonable efforts have been made to publish reliable data and information, but the author and publisher cannot assume responsibility for the validity of all materials or the consequences of their use. The authors and publishers have attempted to trace the copyright holders of all material reproduced in this publication and apologize to copyright holders if permission to publish in this form has not been obtained. If any copyright material has not been acknowledged please write and let us know so we may rectify in any future reprint.

The publisher, the authors and the editors are safe to assume that the advice and information in this book are believed to be true and accurate at the date of publication. Neither the publisher nor the authors or the editors give a warranty, express or implied, with respect to the material contained herein or for any errors or omissions that may have been made.

Trademark Notice: Product or corporate names may be trademarks or registered trademarks, and are used only for identification and explanation without intent to infringe.

ISBN 978-9949-7316-8-8 (Hardback)

ISBN 978-9949-7316-9-5 (eBook)



Authors

Ivan Nazarenko (preface, chapters 1, 2, 3, 4),
Leonid Pelevin, (sections 1.3, 1.4, 4.2),
Oleg Dedov, (section 2.2, 3.3, 4.4),
Oleksandr Kostenyuk (sections 1.5, 1.4, 4.3),
Anatoly Fomin (sections 1.5, 3.1, 3.2),
Mykola Ruchynskyi (sections 3.3),
Anatoly Sviderskyi (sections 2.2),
Yevhen Mishchuk (section 4.1),
Volodymyr Slipetskyi (section 3.3).

Abstract

The monograph is devoted to the development of mechanical systems with dynamic effects on processing media. A new approach and methodology is proposed, taking into account the influence of energy fields of physical and mechanical effects, the transformation and inversion of types of energy exposure. The model of dispersed media under consideration in the range of the process of destruction, grinding and compaction is considered. The revealed changes in the parameters of subsystems: working media, mechanical systems, the processes of their interaction are studied based on the consideration of their stress-strain state. The analysis of combinations and their influence on the intensity of physical and mechanical processes is carried out. The intensification of physical and mechanical processes, methods and means of their creation are achieved by the formulated idea: systematization and complexity of approaches through a joint consideration of the mutual influence of the internal properties of the subsystems made it possible to identify the general laws of their changes and take them into account in the work process. The movement of the working media during high-speed and impact destruction with differentiation of the working area is described. Structuring of the shock process, the formation of entropy destruction, the use of self-organization and the evolution of geometric shapes are evaluated. The process of grinding materials by a vibratory jaw crusher is investigated and methods for determining the effective parameters and their operation modes are proposed. The process of compaction of the processing medium in the field of vibrations in the device with spatial vibrations is described. The laws of change in the device movement, taking into account interaction with the processing medium are established. As a research result, new properties of the behavior of discrete-continuous systems under power load are disclosed. For the first time, stresses and strains are taken into account as working bodies and media for creating energy-saving vibration systems for compaction of building materials. The conducted scientific study makes it possible to obtain the laws of change in the state of dispersed media under the action of power loads by mechanical systems. Minimization of energy costs and increase the efficiency of work processes is proposed when implementing various technological processes.

Keywords

Mechanical systems, technological media, destruction, grinding, compaction, model, parameters, power loads, stresses, deformations, energy, synergetics, vibration amplitude, vibration frequency, laws of motion.

Contents

List of conventions, symbols, units, acronyms and terms	vii
List of Tables	viii
List of Figures	ix
Preface	xi

Chapter 1 Evaluation and analysis of working processes of mechanical systems taking into account the interaction of them from the processing media	1
1.1 Essence of the process of changing the parameters of the dispersed system based on synergistic approaches	1
1.2 Evaluation of methods for describing the processes of energy and mass transfer in dispersed systems	3
1.3 Redistribution of energy flows in the face of intensification of the destruction process of working media and elements of a synergistic connection between the components of this process	10
1.4 Criterion for the minimum energy intensity of the development of working media	12
1.5 The synergistic nature of the interaction of adaptive technical systems with the working medium	13

Chapter 2 Theoretical research of media sealing processes by the technical systems of the construction industry	20
2.1 Investigation of the working process of sealing of construction media	20
2.1.1 Application of similarity criteria for modeling concrete mix with a discrete system	20
2.1.2 Establishment of similarity criteria for modeling a concrete mixture by a continuous system	22
2.2 Investigation of the interaction of aggregate particles with a technical system of vibration exposure	27
2.2.1 Background and assumptions	27
2.2.2 Investigation of the interaction process of particles of aggregate concrete mixture.....	27

Chapter 3 Research of change in the state of dispersed media and technical systems under the action of power loads	35
3.1 Intensification of the energy impact on the working medium in the conditions of shock and vibration shock destruction of soils.....	35
3.2 The general movement of the working bodies of soil-grinding machines and working media as a single synergetic system	43
3.3 Investigation of changes in the operating parameters of two-mass resonant vibrating machines for compaction of construction media.....	47
Chapter 4 Experimental investigations of the motion of mechanical systems taking into account the influence of the media.....	54
4.1 Experimental investigations of operating modes and parameters of the three-mass vibratory jaw crusher.....	54
4.1.1 Experimental device, measuring instruments and research methodology	54
4.1.2 The results of investigations of the influence of design and technological parameters on the crusher efficiency	57
4.2 Experimental investigations of changes in the state of dispersed media in the processes of their development by cutting and impact methods.....	59
4.3 Formation of working processes of soil-grinding machines taking into account the action of physical fields, self-organization and evolution of geometric shapes	64
4.4 Experimental investigations of forming design at dynamic load.....	66
Conclusions	75
References.....	76

List of conventions, symbols, units, acronyms and terms

Exergy efficiency (k_e) – the ratio of input exergy to the original.

Soil density m_1 – mass per unit volume of soil.

Speed of deformation (stress) waves (u) – speed of the front of the disturbance wave in the soil.

Speed of the working body (v) – speed of movement of the working body relative to the working medium.

Stress (σ) – the internal force, which is referred to the unit area at a given section point, is considered.

Working medium – processing material (destruction, cutting, compression, vacuum, welding, gluing, etc.) for which the machine is intended.

List of Tables

4.1 Relative soil erosion

66

List of Figures

1.1	Tooth of the earth moving machine	14
1.2	Working body of the soil disintegrator	15
1.3	Scheme of soil cleavage by the cutting element	16
1.4	Tooth of the earth moving machine	17
1.5	Soil disintegrator tip	18
2.1	Particle motion pattern	29
3.1	Differentiated scheme for determining the power and energy parameters when cutting soils	36
3.2	Dependence of pressures on the front face of the cutting element, normal to the direction of cutting speed, on the depth of cut for loosely bound soils: <i>a</i> – nature of the dependence $\sigma=f(h)$; <i>b</i> – approximation of dependence $P=f(h)$	42
3.3	Pressure distribution on the front face of the cutting element along the width of the tooth $b, \sigma(b)$: <i>a</i> – nature of the dependence $\sigma(b)$; <i>b</i> – approximation of dependence $\sigma(b)$	42
3.4	The dependence of normal stresses in the soil in contact with the front face of the cutting element when cutting cohesive plastic soils: <i>a</i> – nature of the dependence $\sigma=f(h)$; <i>b</i> – approximation of dependence $\sigma=f(h)$	42
3.5	The influence of the cutting angle on the distribution of normal stresses on the front face of the tool (cutting lead) [13]: <i>a</i> – $\delta=100^\circ$; <i>b</i> – $\delta=90^\circ$; <i>c</i> – $\delta=80^\circ$	43
3.6	A fragment of the lateral surface of the working body with the developed elements of differential design	45
3.7	Developed element of differential design	46
3.8	Design schemes: <i>a</i> – with the installation of a vibration exciter on a reactive mass m_1 ; <i>b</i> – with the installation of the vibration exciter on the working body m_2	48
3.9	Amplitude (<i>a</i>) and phase-frequency characteristics and static characteristics (<i>b</i>) of the machine and engine for the circuit (Fig. 3.8, <i>a</i>): $x=0.125$; $\beta_1=0.02$; $\beta_2=0.15$	51
3.10	Amplitude and phase-frequency characteristics and static characteristics of a machine and engine for a circuit (Fig. 3.8, <i>b</i>): at $x=0.125$; $\beta_1=0.02$; $\beta_2=0.15$	53

4.1	Scheme of the physical model of the three-mass vibratory jaw crusher: <i>a</i> – 3D model of three mass vibratory crushers; <i>b</i> – control unit	55
4.2	Experimental device of a vibratory crusher	55
4.3	Schematic diagram of a data acquisition system	56
4.4	Appearance of the data acquisition system	56
4.5	Vibrograms of the third mass of the crusher during its operation with the material ($\omega=75.36$ rad/s, $F=2130$ N, $c_2=219052$ N/m)	57
4.6	Vibrograms of mass oscillations of the crusher during its operation with material ($\omega=104.667$ rad/s, $F=4111$ N, $c_2=219052$ N/m): <i>a</i> – movement of the second mass; <i>b</i> – movement of the third mass	57
4.7	Vibrograms of mass oscillations of the crusher when working with material ($\omega=104.667$ rad/s, $F=4111$ N, $c_2=234438$ N/m): <i>a</i> – movement of the second mass; <i>b</i> – movement of the third mass	58
4.8	Design diagram of the KIBI knocker	60
4.9	Scheme of the device stand for recording the striker movement with teeth upon impact: <i>a</i> – scheme of the device, <i>b</i> – example of recording the dependence $S(t)$	62
4.10	Experimental graphs of the dependence of the average tangential cutting force on the parameters of the shock load	63
4.11	Comparison of the resistance forces of quasistatic and dynamic (impact) cutting versus cut thickness at a constant cutting angle $\delta=45^\circ$	63
4.12	Design 3D model of vibration unit for the formation and compaction of concrete mixtures	67
4.13	General view of the vibration unit	69
4.14	The vibration exciter with unbalance position sensor	69
4.15	Sensor: <i>a</i> – displacements; <i>b</i> – deformations	70
4.16	Layout of measurement sensors	70
4.17	General view of the experimental unit	71
4.18	Oscillogram of vibration unit movement	71
4.19	Oscillogram of the vibration unit movement at an oscillation frequency of 12.5 Hz	72
4.20	Oscillogram of the vibration unit movement at an oscillation frequency of 18.6 Hz	72
4.21	Oscillogram of the vibration unit movement at an oscillation frequency of 24.3 Hz	72
4.22	Deformations of the forming surfaces at an oscillation frequency of 24.3 Hz (sensors 10, 11, 12 (Fig. 4.16))	73
4.23	Deformations of the forming surfaces at an oscillation frequency of 24.3 Hz (sensors 3, 4, 5 (Fig. 4.16))	73

Preface

The processes of deformation of natural and artificial working media have a prominent place in many technological processes of construction, which in the vast majority are dispersed systems. Such processes include the development of soils and rocks, mining, production of construction materials, their processing, as well as the processes of compaction of soil and concrete mixtures and other materials. The most effective ways to carry out such work are those that are based on a dynamic principle of action. Despite the obvious advantages of dynamic deformation, its use is still quite limited. This is primarily due to the lack of theoretical studies of the joint movement of machine units and processing media as a single synergistic system. As a result, in practice, theoretical provisions are applied that do not take into account the features of the dynamic nature of the load and the mutual influence of the subsystems on the general movement. The existing provisions are based on the principles of force deformation, characterized by assumptions that are far from reality: linearization, representation in models of a static application of the deformation force, an assessment of the properties of the medium by empirical coefficients, which are determined without taking into account the load speed and changes in the properties of the medium when changing external loads and propagation conditions in the wave medium deformations and stresses. This approach does not allow taking into account the real physical processes occurring in the working medium with an increase in the intensity of its load.

In this study, a new approach and methodology is proposed for the development of machine systems with dynamic effects on processing media, taking into account the influence of energy fields of physical and mechanical effects, the transformation and inversion of types of energy exposure. Given the versatility of the tasks, criteria have been developed for analyzing combinations and their influence on the intensity of physical and mechanical processes. The intensification of physical and mechanical processes, methods and means of their creation is achieved by the formulated idea: the systematization and complexity of approaches through a joint consideration of the mutual influence of the internal properties of the subsystems will reveal the general laws of their changes and take into account in the work process.

Based on the analysis of literary sources, the main directions of theoretical and experimental studies of the development of processing materials are identified.

A justified model for considering the structural nature of dispersed media in a wide range of all components of the process of destruction, grinding and compaction. The revealed changes in the parameters of the subsystems (working medium, technical systems, processes of interaction of working bodies of primary machinery and machines for grinding and compacting concrete mixtures), taking into account their stress-strain state, is a complex superposition of waves arising in media in disperse systems under the action of dynamic loads. The parameters of the system of soil destruction, grinding and compaction of the media are analyzed and quantitative and qualitative changes of all significant characteristics of the subsystems are revealed.

The dependences for describing the process of compaction of mixtures with a discrete and continuum model and for determining the parameters of resonant vibration systems with directional and spatial vibrations are obtained. The joint movement of the working media during high-speed and impact destruction with differentiation of the working area, structuring of the impact process, the formation of entropy destruction, the use of self-organization and evolution of geometric shapes are described.

A set of experimental studies is carried out according to the developed program at specialized experimental facilities.

The experiments allow to evaluate the results of theoretical studies.

As a result of the studies, new properties of the behavior of discrete-continuous systems under conditions of power vibrations are disclosed.

The obtained laws of changing the state of dispersed media under the influence of power loads by technical systems during the implementation of various technological processes have allowed to propose new load processes, including multi-mode implementation with minimized energy costs and increased efficiency of work processes.

Chapter 1

Evaluation and analysis of working processes of mechanical systems taking into account the interaction of them from the processing media

1.1 Essence of the process of changing the parameters of the dispersed system based on synergistic approaches

In modern scientific research of widespread use, approaches [1, 2] to establish real processes occurring in systems of complex structure, which include technical systems of the construction industry [4], are gaining ground. The energy intensity of the stress-strain state of dispersed materials was considered in our previous works [3–5] and was determined on the stress-strain relationships in the form of a diagram of power loads by various machines that carry out fracture and compaction processes. This approach determines the energy intensity of the process for one period of interaction of two subsystems. The total energy of the process in [5] was determined taking into account the total time of concrete compaction technology:

$$E = \bar{E}Vt_n/T, \quad (1.1)$$

where \bar{E} – the specific energy spent on compaction of a unit volume V over a period T ; t_n – duration of the process.

The application of dependence (1.1) requires an exact experimental value \bar{E} ; in [5] it is determined as follows:

$$\bar{E} = \bar{E}_0 \frac{(K_E - 1)}{K_E \ln E_K}, \quad (1.2)$$

where \bar{E}_0 – energy in the initial period of compaction; $K_L = \bar{E}_0/\bar{E}_K$ coefficient determining the change in the deformation diagram (hysteresis loop) during compaction.

The approach used in [2] is also based on the determination of the stress-strain state in the form:

$$\sigma_{st} = \rho A / \varepsilon_{rel} t, \quad (1.3)$$

where σ_{st} – stress, N/m²; A – energy constant of the material, N·m/kg; ρ – density of the material, kg/m³; ε_{rel} – relative deformation of the structure of the material.

The reason for the dependence (1.3) in [2] used the well-known mechanics of determining power $P = E/t$ (E – energy, t – time):

$$\varepsilon dm = KPdt, \quad (1.4)$$

where ε – specific energy absorption per unit of production, J/kg; m – the amount or mass of the processed material, kg; P – power consumed by the machine per unit, J/s.

The parameter εdm determines the energy intensity of the process. This parameter is a qualitative indicator of the process. The indicator εdm also changes with a change in the state of the medium, as well as a possible change in the operating parameters of a technical object (technological process machine). The mass indicator dm and volume dV is a quantitative indicator of the process.

It is worth noting that dependence (1.4) estimates only the component of the total energy balance of the system, goes to make changes in the state of the dispersed medium, and does not take into account other energy expenditures (for example, friction).

This approach has been tested on the energy intensity of the working process of moving cargo by various types of vehicles [2]. It is worth noting that this approach does not disclose the complexity of the phenomena that occur during the interaction, for example, systems of technical objects that carry out the processes of destruction, mixing and compaction, which is the subject of these studies.

It is obvious that the development of the synergetic concept consists in the use of unbalanced thermodynamics, on the basis of which optimization principles have been developed, which can be used for the studied processes of technical systems of the construction industry. Let's consider the defining notions of unbalanced thermodynamics with a preliminary definition of synergetic fundamentals in processes and technologies.

Synergetics is a phenomenon that certifies the transition from an unstable (spontaneous, chaotic) state of a structure (material, process, etc.) to an ordered state [2] due to the joint (targeted) action of subsystems in the general movement of a certain (studied) system. So, synergetics determines the conditions for the self-organization of a structure over time, consisting of simple studied subsystems to a complex, already ordered (completed)

structure, which must be achieved as a result of interactions between sub-systems. From the standpoint of synergetics, the energy seemed to «freeze» in the form of crystalline structures, transforming from kinetic to potential energy. In other words, a substance is a frozen energy spent not only on mechanical, but also on the creation of new stable structures in the processes of compaction of materials and other technological processes.

So, as a brief description of synergetics as a scientific paradigm, it is possible to use the key ideas underlying it: self-organization, open systems and non-linearity.

Thus, synergetics studies open non-equilibrium systems that are capable of self-organization through the exchange of matter, energy and information with the surrounding continuum. Moreover, a decrease in the entropy of any system within the framework of its equilibrium requires an influx of non-entropy, that is, an increase in entropy outside the system under consideration.

1.2 Evaluation of methods for describing the processes of energy and mass transfer in dispersed systems

The energy supplied from the working body of the machine is an outstanding parameter of any system, and the change in energy and entropy in the system is accompanied by changes in its parameters, which, in turn, can be accurately described by the rules of synergetics (energy entropy), which can be considered in accordance with the working process. The following provisions and definitions apply.

1. Any material system can't function, and not consuming the energy ΔE , spent on the work A , to change the internal energy E_{in} and to dissipate heat in the medium E_d :

$$\Delta E = E_{in} + A + E_d. \quad (1.5)$$

Work A is spent on changing the state of the system (creating a stress state in the structure of a substance).

2. Really isolated systems tend to spontaneously switch from less probable states to more probable, that are, from ordered to less ordered. In this case, the entropy increases according to the law:

$$S = k \cdot \ln A, \quad \Delta S = S_2 - S_1 \geq 0. \quad (1.6)$$

For all real non-equilibrium and irreversible systems, condition ($>$) condition ($=$) is true for ideal inverse processes and systems [2]. The rate of increase in entropy $\Delta S/\Delta t$ is determined by the irreversibility degree of the processes. In accordance with this, the law of increasing entropy:

$$\frac{\Delta S}{dt} \geq \frac{1}{T} \int j_i dx_i, \quad (1.7)$$

where j_i – the energy flows to the input of the medium-working organ system;

$$A_{AD} = \phi \Delta b \int \int_{G_1} \sigma_1(x, z) dx dz,$$

are entropic driving forces of resistance arising on the working body.

In isolated systems, entropy increases, and negentropy decreases. So, negentropy characterizes the quantity and quality of energy at the entrance to the system, and the above equation expresses the pattern of energy consumption. Therefore, a system that performs mechanical work can be considered as a source of negentropy (vibration platform frame, concrete mixer drum). Therefore, the drive system of machines and mechanisms can be considered as a source of negentropy.

3. The progressive development of systems determines the rule of entropy content in open systems. The entropy of open systems in the system of their progressive development is always reduced due to energy consumption from external sources. For this case, the entropy of external systems is increasing. It follows that any external influence is due to the expenditure of energy and the growth of the entropy of external systems.

4. Material systems with progressive development (mixing, compaction, destruction, etc.) reach the limit that can be expressed by the maximum values of the corresponding level of entropy ($-\Delta S_{\max}$). Therefore, to achieve technological requirements in interacting systems, there is a minimum of energy to obtain maximum product quality or production result.

Such a statement in achieving technological results is important for improving the design of machinery and equipment, optimizing the parameters of deformation of materials, etc.

If, under the influence of the working body on the medium, internal effects arise in it, the state of which, together with the energy sink, are in conditions of local thermodynamic equilibrium within the variation of the entropy of the system and are characterized by dS/dt .

Then the total entropy S associated with external and internal processes in local volumes in accordance with [1] is described by the equations:

$$\frac{d_e S}{dt} = -\oint J_s dF; \quad \frac{d_i S}{dt} = \int \sigma dV, \quad (1.8)$$

where $d_e S$ – inflow of entropy from the side of the working body; $d_i S$ – change in entropy within the system associated with physicochemical transformations in the system; J_s – density of the substantial influx of entropy;

σ – production of entropy (stress in the medium, or stress on the working body of the machine); dF – surface of the interface.

Taking into account that $dS = d_e S + d_j S$ it is possible to write:

$$\frac{dS}{dt} = \frac{\sum_{j=1}^{j=R} A_j J_j + A_q X_q + \sum_{k=1}^{k=1k} J_k X_k + P^v X_v + P^w X_v^a + \frac{P^a S}{X_v} - \nabla J_q + \sum_{k=1}^{k=1k} \mu_k J_k}{\rho T}, \quad (1.9)$$

where A_j, X_q, X_v^a, X_v^S – some thermodynamic forces having the following meaning: chemical affinity A_j for the j -th reaction of the component:

$$A_j = \sum_{k=1}^R \mu_k \nu_{kj}, \quad j = 1, 2, \dots, R.$$

It is represented as a scalar thermodynamic force conjugate to the rate of the j -th reaction.

Wherein:

$$J_j = \frac{1}{\gamma_{kj}} \frac{d\rho_k}{dt}, \quad (1.10)$$

where X_q – polar vector:

$$X_q = -\frac{\nabla T}{T} = \nabla \ln T,$$

which is the thermodynamic force of thermal conductivity for a certain heat movement J_q .

Thermodynamic diffusion forces associated with the diffusion flux density:

$$X_k = F_k - T \nabla \left(\frac{\mu_k}{T} \right) \quad (1.11)$$

ensuring the creation of stresses in the medium due to the flow of energy.

$X_v \equiv -\nabla V$ – scalar astrigent force, conjugated with pressure as a stream of momentum.

$X_v^S \equiv -(\nabla V)^S$ – tensor viscosity force, which causes the phenomenon of viscous shear under the action of pressure.

$X_v^a \equiv -(\nabla^v - 2\omega)$ – thermodynamic power of irreversible effects.

A comparison of (1.9) with (1.8) shows that the substantial density of the entropy flux J_s is determined by the second and third terms of equation (1.9):

$$J_s = \frac{J_q - \sum_{k=1}^k \mu_k J_k}{\rho T}, \quad (1.12)$$

and entropy production σ or energy dissipation determines the first term of the equation, i. e.

$$\rho T \sigma = \left[\sum_{j=1}^R A_j J_j + J_q X_q + \sum_{k=1}^k J_k X_k + P^v X_v + P^w X_v^a + \frac{P^{as}}{X_v^s} \right]. \quad (1.13)$$

The value $(\rho T \sigma)$ determines the amount of energy dissipated or absorbed by the system as a result of the action of the working body of the machine and the course of internal processes in the system observed during technological distributions (destruction and compaction of materials).

Equations (1.8), (1.9) can describe any combination of complex irreversible processes. For this, it is necessary to set the boundary conditions and determine the set of adequate thermodynamic functions, as well as the parameters of the input and output of the system in accordance with the mechanisms of action of the machine on the processing medium (destruction, mixing, compaction).

The first historically known mathematical problems (Sumer, China, India, Egypt) belonged to the field of geometry and were associated with the determination of distances for specific conditions. In form, these tasks were poetry miniatures, and their solution did not involve the use of any symbolism (notation, numbers) and was completely based on the methods of logical thinking. Two thousand five hundred years ago, Plato took a big step in the development of the theory of knowledge, introducing such a concept as the image («idea») of an object. At first, this method was applied to describe the geometric shape of real objects. For example, the concept of «circle» can still be applied to the shape of the visible sun, chariot wheels, shields, dishes, etc., regardless of the fact that all these objects are fundamentally different.

The scientific and methodological basis for describing the processes of energy and mass transfer is the concept of field. The concept of «field» describes the distribution of a scalar quantity, for example, temperature (K) or the concentration of a substance (kg) in space, that is, depending on another scalar quantity – linear size. Such a field is called stationary and it can be represented in general form as:

$$\begin{cases} t = t(x, y, z); \\ C = C(x, y, z), \end{cases} \quad (1.14)$$

where t – temperature, C – concentration; x, y, z – Cartesian coordinates.

If, in addition to this, the change in the scalar quantity in time is considered, then the field is called non-stationary, and the dependences are of the form:

$$\begin{cases} t = t(x, y, z, \tau); \\ C = C(x, y, z, \tau), \end{cases} \quad (1.15)$$

where τ – time.

For the mathematical description of mechanical processes in systems of material bodies and media, the concept of «vector field» is used, for example, the field of velocities and accelerations:

$$\begin{cases} \bar{w} = \bar{w}(x, y, z); \\ \bar{a} = \bar{a}(x, y, z), \end{cases} \quad (1.16)$$

for stationary fields and

$$\begin{cases} \bar{w} = \bar{w}(x, y, z, \tau); \\ \bar{a} = \bar{a}(x, y, z, \tau), \end{cases} \quad (1.17)$$

for non-stationary fields, where w – speed; a – acceleration.

Equation (1.16) and (1.17) are the most complex, since three scalars (projections on the coordinate axis) must be used to describe one vector quantity.

As an example, let's consider the basic equations that describe the distribution of temperatures, concentrations, and accelerations in the moving material.

Energy equation:

$$\frac{Dt}{\partial \tau} = a \cdot \nabla^2 t. \quad (1.18)$$

Fick's diffusion equations:

$$\frac{Dt}{\partial \tau} = D \cdot \nabla^2 c. \quad (1.19)$$

Navier-Stokes equations (projected onto the X axis):

$$\frac{Dw_x}{d\tau} = g_x - \frac{1}{\rho} \nabla P + \nu \nabla^2 w_x. \quad (1.20)$$

In the equations (1.18) – (1.20) on the left side are the so-called full (substantial) derivatives of scalar quantities:

$$\frac{Dt}{d\tau} = \frac{\partial t}{\partial \tau} + w_x \frac{\partial t}{\partial x} + w_y \frac{\partial t}{\partial y} + w_z \frac{\partial t}{\partial z}, \quad (1.21)$$

$$\frac{Dc}{d\tau} = \frac{\partial c}{\partial \tau} + w_x \frac{\partial c}{\partial x} + w_y \frac{\partial c}{\partial y} + w_z \frac{\partial c}{\partial z}, \quad (1.22)$$

$$\frac{Dw_x}{d\tau} = \frac{\partial w_x}{\partial \tau} + w_x \frac{\partial w_x}{\partial x} + w_y \frac{\partial w_x}{\partial y} + w_z \frac{\partial w_x}{\partial z}. \quad (1.23)$$

Equation (1.21) – (1.23) consists of determinants (their form is unique) that describe the change in temperature t , concentration c and speed in time (the first terms on the right side of the equations) and in coordinates (x, y, z) , and the coordinate system itself moves at a speed whose components are the projections w_x, w_y .

The right-hand side of equations (1.18) – (1.20) presents factors affecting the formation of temperature and concentration fields:

$$\nabla^2(A).$$

Designation by $\nabla^2(A)$ is the Laplace operator with respect to the scalar (A) :

$$\left\{ \begin{array}{l} \nabla^2 t = \frac{\partial^2 t}{\partial x^2} + \frac{\partial^2 t}{\partial y^2} + \frac{\partial^2 t}{\partial z^2}; \\ \nabla^2 c = \frac{\partial^2 c}{\partial x^2} + \frac{\partial^2 c}{\partial y^2} + \frac{\partial^2 c}{\partial z^2}. \end{array} \right. \quad (1.24)$$

The coefficients a and D in equations (1.18) – (1.19) are classified as thermophysical constants (tabulated values): $\alpha = \lambda / c_p \rho$ – coefficient of thermal diffusivity; c_p and ρ – isobaric heat capacity and density of the medium, respectively; D – diffusion coefficient; λ – coefficient of thermal conductivity.

Similarly, in equation (1.20), the formation of the speed field is determined by the action of viscosity forces:

$$v \cdot \nabla^2 w_x = v \cdot \left(\frac{\partial^2 w_x}{\partial x^2} + \frac{\partial^2 w_x}{\partial y^2} + \frac{\partial^2 w_x}{\partial z^2} \right), \quad (1.25)$$

where v – thermophysical constant – kinematic coefficient of viscosity (tabular value).

In addition, the formation of the speed field is affected by gravity (gravitational constant) and pressure forces.

If consider the movement of a concrete mixture, which is represented by a viscous fluid, when the speed field is formed mainly by the mani-

festation of viscosity forces, then equations (1.18) – (1.19) can be represented as:

$$\begin{cases} \frac{Dt}{\partial\tau} = a \cdot \nabla^2 t; \\ \frac{Dc}{\partial\tau} = D \cdot \nabla^2 c; \\ \frac{Dw_x}{\partial\tau} = a \cdot \nabla^2 w_x. \end{cases} \quad (1.26)$$

Equations (1.18) – (1.20) belong to the category of equations of mathematical physics and are the most complex in the mathematical description of technological processes [5].

The transition from differential equations to equations in generalized variables is based on the theory of similarity [3], which allows to describe a whole class of similar processes in a single mathematical form, the concrete form of which is established by the results of processing experimental data. These equations, as a rule, have the form of power dependencies.

The main working dependencies that make it possible to carry out verification and constructive calculations of energy and mass transfer processes are the following equations:

– specific heat flux:

$$q = \frac{\lambda}{\delta} \cdot \Delta t = \alpha \cdot \Delta t; \quad (1.27)$$

$$q = k \cdot \Delta t \left[\frac{\text{W}}{\text{m}^2} \right] \text{ or } \left[\frac{\text{J}}{\text{s} \cdot \text{m}^2} \right];$$

– specific mass flow:

$$\bar{m} = \beta_c \Delta p = \beta_p \Delta P_n \left[\frac{\text{kg}}{\text{cm}^2} \right]. \quad (1.28)$$

Pressure losses during transportation of the mixture with stirring:

$$\Delta p = c_t \frac{p\omega^2}{2} \left[\frac{\text{N}}{\text{m}^2} \right], \quad (1.29)$$

where λ – coefficient of thermal conductivity, $[\text{W}/\text{m} \cdot \text{K}]$ – tabular value; Δt – current temperature difference in the system; α, k – heat loss and heat transfer coefficients, respectively $[\text{W}/\text{m}^2 \cdot \text{K}]$; β_p, β_c – mass transfer coefficients for pressure and concentration, respectively ($\beta_c = \beta_p / RT$;

$\beta_c = \beta_p/RT$); c_t – resistance coefficient; Δp – density difference in the process of mass transfer.

Knowing the numerical values m , it is possible to determine the integral characteristics of the process of heat and mass transfer.

The amount of energy transmitted:

$$Q = qS\tau[J]. \quad (1.30)$$

Transfer mass:

$$M = \bar{m}S\tau. \quad (1.31)$$

Transfer power:

$$\underline{P} = \frac{\Delta p}{\eta} [W]. \quad (1.32)$$

Here S – surface with a mass of energy exchange, $[m^2]$; τ – process flow time, $[s]$; V – volumetric flow rate of the system, $[m^3/s]$.

Dependencies (1.27) – (1.32), like equation (1.18) – (1.26), form the basis for developing a mathematical model of the investigated systems.

1.3 Redistribution of energy flows in the face of intensification of the destruction process of working media and elements of a synergistic connection between the components of this process

The intensification of the destruction process of working media is the most effective method of increasing the efficiency of soil development. At the same time, not only the energy intensity of the destruction of the working medium is reduced, but also all the specific parameters of the equipment for the destruction of the soil and its working processes are significantly improved, and the technogenic load on the medium is also reduced.

According to the dynamic fracture, not only the kinematic parameters of the interaction of the working bodies with the working medium fundamentally change, but also the characteristics of the working medium and the physics of the interaction of destructive elements with the soil. The stress-strain state acquires an oscillatory-wave character, which is a superposition of direct, reflected and refracted stress waves (deformations) arising from the action of a destructive element on the soil, vibrations

of soil particles and waves resulting from these vibrations. With such a complex nature of the stress-strain state, even with compressive actions of destructive elements in the soil, regions with tensile stresses can occur, which can be centers of destruction, because the tensile strength of soils is much less than the compressive strength. Significantly change the characteristics of the working medium (quantitatively and qualitatively), depending on the speed of application of loads. The dynamic ultimate strength of the soil increases.

For compressive stresses $\sigma_{c.d.} = k\sigma_c$; $\sigma_{c.d.}$ – the limit of the dynamic tensile strength of the material under compression; σ_c – ultimate strength of the material under compression; k – coefficient of dynamic strength ($k=1.3\dots1.6$). Through other static strength cutting $\sigma_c = 4.77m_v$; $c = 1.52m_v$; $\sigma_{c.d.} = (6.2\dots7.63)m_v$ and $\sigma_{c.d.} = (4.09\dots5.04)c$, where m_v – the specific strength of the soil of destruction in the frontal part of the slot along the cutting angle $\delta=45^\circ$; c – adhesion.

The volume of plastic deformations is significantly reduced up to their complete absence. Failure becomes brittle and at the same time the value of the relative ultimate dynamic deformations decreases by an order of magnitude or more with respect to the relative ultimate static deformations.

The array of working medium parameters is expanding, it is poured onto the fracture process, namely: the rate of interaction of destructive elements with the working medium, the propagation speed of stress waves (strains) in the working medium, soil density, elastic modulus, Poisson's ratio, soil compressive and tensile strength limits, ultimate relative deformation, amount and magnitude of loads on soil volume until its complete destruction, endurance limit on various types of stresses.

A very important factor for increasing the efficiency of soil destruction is the formation of energy flows and their redistribution in space and time, that is, its maximum direct alignment with the cutting (impact) edge.

It should be noted that the natural development of systems of any kind occurs according to general principles that are studied by interdisciplinary science – synergetics, which studies the general laws of phenomena and processes in complex non-equilibrium systems based on their inherent principles of self-organization.

Systems due to the combined actions of their components and their reactions to external influences lead to the emergence of spatial, temporal or spatio-temporal structures. Systems in which synergistic processes occur are inherent in such properties as non-linearity, openness, dissipativity.

Nonlinearity determines the power of the response of the system to an external action, which (power) depends not so much on the magnitude of the external energy action, but mainly on the qualitative nature of this energy effect.

Dissipativity is selective in nature, which leads to the attenuation of those processes that do not correspond to the laws of system development.

In systems providing processes for the destruction of working media, their development is ensured by the implementation of certain constituent elements of synergetics. Certain adaptive relationships between the elements of the system are implemented on the basis of direct and feedbacks of a positive and negative nature. This nature of the functioning of the soil-grinding systems allows to increase the efficiency of the soil development process.

Separately, it should be noted that synergetic principles should be studied and applied already at the stages of the formation of ideas, design and manufacture of technical systems and the formation of their working processes. Thus, a scientist, engineer, and worker become creative «components» of a single natural synergetic process in organizing and developing processes for developing working media such as those that harmoniously fit into the existence of the natural medium.

1.4 Criterion for the minimum energy intensity of the development of working media

Working media are developed by technical systems of soil cultivation equipment, represented by natural and artificial soils. Structurally, soils belong to disperse systems, they are defined as heterogeneous systems consisting of two or more phases with a developed interface between them. One of the phases forms a continuous dispersion medium (gas, liquid, solid), in which the dispersed phase is distributed in the form of small solid particles, liquid droplets or gas bubbles. Strong natural (coarse, half-rock and rocky) and artificial (concrete, brick, etc.) media consist of a solid dispersion medium and a solid dispersed phase, and under specific conditions with gaseous and liquid dispersed phases. All the rest are from a solid dispersion medium and liquid and gaseous dispersed phases.

The processes of interaction of technical systems with dispersed working media appear to be occurring in space and time. This interaction is characterized by power and energy flows directed by the working bodies of the soil-grinding machines to the soil with the aim of destroying them with certain output parameters. A general condition for ensuring increased soil destruction efficiency by technical systems is the intensification of the working processes of these systems. When constructing physical and mathematical models of the intensification of the processes of destruction of working media, it is necessary to take into account that depending on the speed of application of the load on the soil, their parameters change significantly (qualitatively and quantitatively) and radically affect the nature of the processes of soil destruction.

As indicated, the output parameters of the dynamic process of the destruction of working media by technical systems depend on two parame-

ters of time t and distance x , the physical and mathematical model of these processes is represented by a system of differential equations with separate derivatives.

The formation of dynamic work processes of technical systems based on physical and mathematical modeling should meet the criteria of optimality. The most common are energy and exergy criteria that determine the effectiveness of the design of machines and work processes. These criteria determine the energy efficiency for the production of a particular product. Other criteria, for example, on the productivity of material consumption, rigidity, accuracy, power, etc. are derived from energy and exergy criteria.

When comparing the effectiveness of technical systems of the construction industry, the rational use of energy and the optimal orientation of flows are determined on the basis of the overall efficiency, energy intensity $E = P/m$ (W/J), which determines the amount of energy flow per unit of transferred substance or energy, exergy efficiency, where E_{in} , E_{out} – exergy of input and output flows, thermodynamic efficiency, $k_t = E_u/E_e$, where E_u , E_e – exergy that is actually used, and exergy is evident.

Thus, the general criterion for the assessment of physical and mathematical models, on the basis of which the designs of technical soil-grinding systems are developed and their work processes are formed, is the minimum energy intensity of the development of working media.

1.5 The synergistic nature of the interaction of adaptive technical systems with the working medium

In the development of soils and rocks, mining, construction materials, their manufacture and processing, a significant place is occupied by the processes of deformation and compaction of working media. According to an integrated and systematic approach, these processes are studied as systems consisting of three significant elements of the complex, namely: working media, technical systems and the processes of their interaction. In addition, environmental influences on all elements of the complex are taken into account.

To determine the deep connections between the components of the complex, all its elements are considered as forming a single synergetic system. When this system moves, a dynamic interaction of the elements of the complex occurs, direct and inverse relationships between the elements are formed. In this case, these relations can be both negative and positive. Adaptation processes between the elements of the complex are also organized during the movement of systems that determine the quantitative and qualitative nature of this movement.

The principles of constructing structural, geometric, kinematic, spatial and temporal features of the working bodies of technical systems in

a synergetic sense allow optimal organization of technological processes of technical systems.

It should be noted that the formation of technical systems and their work processes based on synergetic principles gives the highest possible efficiency. In the synergetic sense, the connections between the elements of the complex have a wide spectrum in qualitative and quantitative character.

Considering the power parameters of the destruction of the working medium, it should be noted that the adaptive connection «working body — working medium — cutting forces» can be implemented in various ways, depending on the design of the destructive element.

In the tooth structure of an earth moving machine, developed at the Kyiv National University of Civil Engineering and Architecture (KNUCEA) (Fig. 1.1), the machine's functioning efficiency is improved by adaptive automatic departure control. The tooth contains a riser 1 and tips 3, 4.

The tips of the tooth are made in the form of wedges interconnected by a crossbeam 2. An elastic element (EE) is installed inside the tooth. Tips 3 and 4 are mounted with the possibility of longitudinal movement relative to the crossbeam, for which they and the crossbar have grooves. When a tooth encounters during work with strong soils, the tangential cutting force P_t increases, and together with it the lateral (transverse) P_l force (the tooth has a dihedral design); EE is deformed due to the side reaction force of soil resistance to fracture and the tips approach each other at a certain distance. Thus, the width of the excavation is reduced, respectively, the tangential cutting force is reduced, it allows to continue the development of the soil without reducing the depth of cut, excluding the actions of the operator to perform certain control operations.

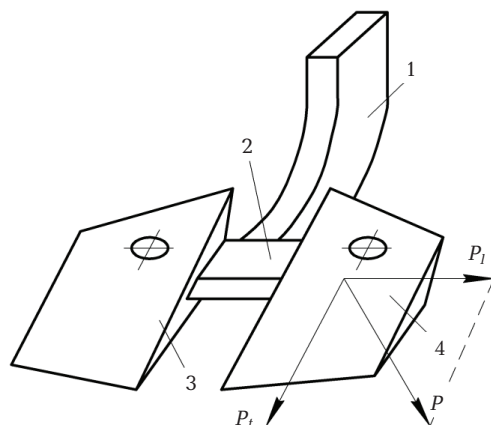


Fig. 1.1 Tooth of the earth moving machine

An even wider connection between the values of the resistance of the working medium to destruction and the adaptive response of the working body of the technical system is implemented in the following technical solution of KNUCEA (Fig. 1.2). The working body has the ability to change the geometry of its structure in a wide range, which is an adaptive response to a wide range of strength soil characteristics.

The adaptive connection «working body – working medium – destruction intensification» reduces the energy consumption of soil development.

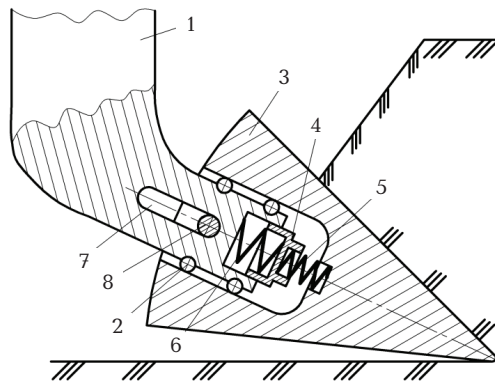


Fig. 1.2 Working body of the soil disintegrator

The working body of the soil disintegrator contains a riser 1, a tip 3 and a shock absorber, which is a glass 4 with sockets in which the working 5 and safety 6 springs are placed. The maximum elastic force of the safety spring is equal to the permissible elastic force in the dangerous section of the riser 1. As a result of the resistance of the soil to cutting, the tip 3 with finger 8 slides into the groove 7, moving into the soil relative to the riser along the roller bearings 2, compressing the working spring 5. Installation of working spring between the riser and the tip provides a smooth load of the riser and reduce peak loads on the working equipment. In addition to reducing dynamic loads on the riser, the working spring acts as an intensifier of the impact on the working medium. Storing energy during the movement of equipment in the soil, it intensively releases it during a large cleavage of soil.

Such a technical solution intensifies the process of soil destruction due to spring elements that accumulate energy from the engine of the machine during its movement (dependent activation). The most effective independent activation, when a separate reason for the dynamic destruction of the working medium is directly established on the working body.

The working process of the soil disintegrator with independent activation is carried out by deepening the tip fixed on the rack into the soil. The value of the step of soil cleavage are found by the formula (Fig. 1.3):

$$l_{cl} = (hk_h - a)(ctg\delta + ctg\theta),$$

where h – depth of cut; k_h – coefficient taking into account the depth of contact of the cutting element with the soil at the time of cleavage of a large soil element; a – cut value of the side edge of the cutting element; δ – cutting angle; θ – angle between the path of the cutting element and the prevailing direction of movement of the isolated pieces of soil.

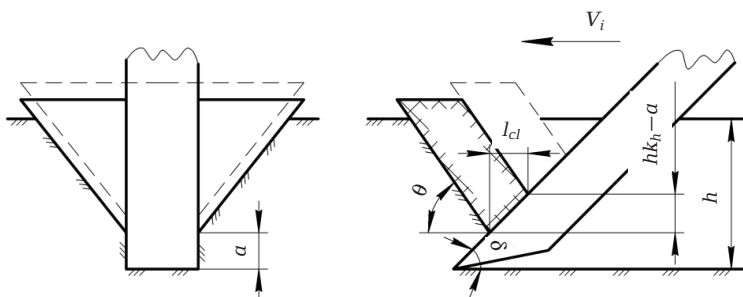


Fig. 1.3 Scheme of soil cleavage by the cutting element

The cut value of the side edge of the cutting element is found by the formula:

$$a = h(1 - k_{side}),$$

where k_{side} – depth factor of the part of the opening expands.

The value of the angle between the path of the cutting element and the prevailing direction of movement of the cleavage is found from the following expression:

$$\theta = \frac{\pi}{4} - \frac{\rho}{2},$$

where ρ – the angle of internal friction.

The coefficients k_h and k_{side} are determined experimentally.

One of the important features that occur during the development of soils is the mandatory wear of the cutting elements. At the same time, a wear area appears on the cutting element at a negative angle to the cutting path, increasing the support of the soil when cutting. When the working body is shortened during operation to a certain (critical) value, the wear

area increases as much as possible, that is, the angle between the tangents to the front and rear faces increases, which leads to a significant increase in the energy intensity of soil cutting. Taking into account the above, the tooth design of the digging machine was developed at KNUCEA (Fig. 1.4).

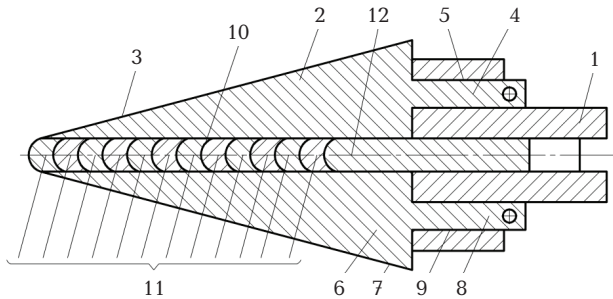


Fig. 1.4 Tooth of the earth moving machine

Tooth 1 consists of the upper part 2 with the front face 3, the shank 4 installed in the groove 5 of the tooth, the lower part 6 with the rear face 7 and the shank 8, installed in the groove 9 of the tooth, and the main working part 10 made of a set of capacious elements of the components of the wear body 11 are made so that the inner surface of the first wear body is an exact copy of the outer surface of the second wear body, and the inner surface of the second wear body is a copy of the external surface of the third wear body, etc. The wear body is located between the outer and inner surfaces. The outer surface is congruent to the inner, that is, the wear body is a repetition of each other and thus, sealed together, makes up the main working part with the tip 12, which is located between the upper and lower parts. The tip is inserted into the pocket 13 of the tooth. The wear bodies will replace each other and during the entire time of operation the cutting part of the tooth will have an optimal shape and will form under real conditions of the wear process.

Another technical solution (Fig. 1.5) has such a feature that, with wear, the element in the area of the cutting edge is replaced. The tip of the soil disintegrator contains side faces 1 with mounting holes 2, front 3 and rear 4 faces with longitudinal slots and a variable cutting element. The slots are made along the perimeter of the longitudinal faces of the tip and flexible elements from the locking device are placed in them.

The replaceable element is made in the form of a set of plates 5, which are interconnected by end edges and mounted on a tape. Each of the plates in cross section has the shape of a parallelogram. A smaller face of the front plate is placed in the same plane as the front face of the soil disintegrator tip. The length of the edges of each plate attached to the tapes corresponds to the given expression:

$$l = h(\operatorname{ctg}(\alpha + \gamma) + \operatorname{ctg}\beta),$$

where h – thickness of the cutting element; β – tip sharpening angle; γ – angle between the rear face of the tip and the horizontal plane; α – angle between the smaller diagonal of the parallelogram of the plate and the horizontal plane.

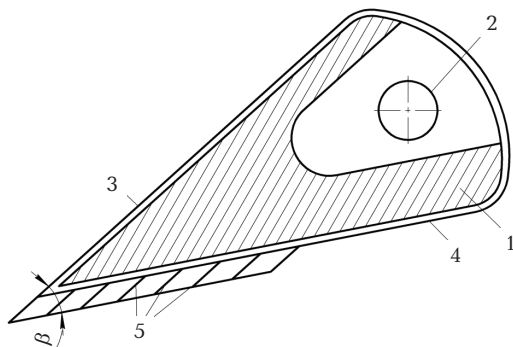


Fig. 1.5 Soil disintegrator tip

When deepened, the tip destroys the soil. Addendum on the end edge of the front plate contributes to the development of cracks in the soil in the direction of movement of the tip, helps to reduce the energy consumption of soil development. The proposed automatic maintenance of the necessary shape of the cutting edge of the tooth in the cutting zone occurs during the entire period of its operation.

An important element in ensuring the effectiveness of the process of soil destruction is the choice of height of the cutting insert. The height of the cutting insert is determined from the dependence:

$$\Delta h = (1 - k_{side})h_t,$$

where Δh – height of the cutting insert; k_{side} – coefficient of the expanded part of the opening; h_t – tooth height equal to the depth of cut.

This size of the cutting part provides the least energy-intensive separation of the soil from the soil body as the lateral expansion of the openings with this size of the cutting part have the greatest specific value in the cross section of the opening. The cross-sectional area of the middle part of the opening and the length of the cutting edge of the knife or tooth should be minimal within the permissible limits. The outline of the edge of the bucket visor should be close enough to the outline of the side surfaces of the soil opening. These conditions are met by cutting the soil with a bucket or

a cutting part of the minimum height Δh at a given cutting depth h_i , ensuring the free distribution of the lateral extensions of the opening to the surface of the soil body. The communication angle of the side walls of the plate has a symmetrical angular shape with branches diverging at an angle $\pi - 2\gamma$, where γ – angle of inclination of the side surfaces of the openings in the soil during their natural formation. The cutting insert is located in the corner joint of the insert walls, and the immersion depth is equal to its height. Due to this, the side and front walls do not interact with undestructed soil, therefore, the cutting insert can be made of minimal thickness, allows soil to be destroyed, thereby reducing the metal content of the parts, wear out, and reducing the wear area, and therefore reducing the resistance of the soil to cutting and increasing productivity development of work media.

Thus, taking into account the natural connections between elements that are synergistic in various aspects of the interaction between the iconic components of the complex that make up the system for developing working media, can significantly reduce the energy consumption of a given technological process.

Chapter 2

Theoretical research of media sealing processes by the technical systems of the construction industry

2.1 Investigation of the working process of sealing of construction media

2.1.1 Application of similarity criteria for modeling concrete mix with a discrete system

Theoretical studies are based on the consideration of the working process with a preliminary assessment of the influence degree on the efficiency of the working process of processing construction media. The obtained results open up the possibility for calculating the characteristics and parameters of the working process, for the perfect determination of the design features of technical systems of the construction industry. The problem is formulated as follows. The vibration system with the parameters is set: the amplitude of the oscillations x_0 and the frequency of the vibration effect ω ; the mass of particles in the mixture has a density ρ and an average size r ; average speed v relative to the vibrating working body; the friction force F_{fr} , which occurs between particles during vibrations, is proportional to the square of the linear size.

It is necessary to determine the value of a certain set of parameters of the vibration system that provides the greatest value of the compaction coefficient of the construction medium with limited values of specific work \bar{A} and specific power \bar{P} :

$$\bar{A} = \frac{1}{2} x_0^2 \omega^2; \bar{P} = \frac{1}{A\pi} x_0^2 \omega^3. \quad (2.1)$$

The initial parameter is the sealing coefficient:

$$K_s = \frac{\rho - \rho_0}{\rho} \cdot 100 \% = \rho_c.$$

Thus, the overall functional dependence has the form:

$$\rho_c = f(m_c, r, x_0\omega, F_{FR}, t, g, \bar{A}, \bar{P}).$$

Using the dimensional method, let's obtain:

$$\rho_c = f\left(\frac{F_{FR}}{m x_0 \omega^2}; \frac{v}{x_0 \omega}; \omega t; \frac{x_0 \omega^2}{g}; x_c^2 \omega_c^2; x_c \omega_c^3\right). \quad (2.2)$$

Here $F_{FR}/m_c x_0 \omega^2$ and $v/\alpha \omega$ characterize the resistance, respectively, of forces and velocities; other options are restrictive. Obviously,

$$F_c \frac{F_{FR}}{m x_0 \omega^2} = \frac{\mu r^2}{k \rho r^2 x_0 \omega^3} = \frac{\mu_1}{\rho r \omega v}, \quad \mu_1 = \frac{\mu}{k}, \quad k = \frac{4}{3} \pi, \quad (2.3)$$

that is, the ratio of the friction force (μ – coefficient of proportionality) to the vibrational force acting on the particle m is inversely proportional to the density of the medium ρ , the amplitude of the excitation speed v of the particle size r and frequency ω .

A measure of process efficiency can be taken:

$$K_v = \frac{U}{V} = \frac{U F_c \rho r \omega}{\mu}. \quad (2.4)$$

Hence:

– at $U = v$:

$$K_v = 1, \quad F_c = 0 \quad (F_{FR} = 0);$$

– at $U = 0$:

$$K_v = 0, \quad F_c = 1 \quad (F_{FR} = m x_0 \omega^2);$$

– at $U F_{dr} \rho / \mu = \text{const} = C$:

$$K_v = C r \omega.$$

Therefore, to achieve the same efficiency of the vibration process while reducing the size of the aggregate particles, it is necessary to increase the oscillation frequency of the working body ω .

It is interesting to compare the friction force with the particle weight:

$$\frac{F_{FR}}{m g} = \frac{\mu r^2}{m g} = \frac{\mu r^2}{k \rho r^3 g} = \frac{\mu_1}{\rho g r}, \quad (2.5)$$

that is, the ratio of the friction forces acting on the particle to its weight is inversely proportional to the density ρ and particle size r . The ratio of inertia and particle weight:

$$\frac{m x_0 \omega^2}{mg} = \frac{x_0 \omega^2}{g} = n \quad (2.6)$$

represents an important criterion that determines the ratio of the effective acceleration and gravitational acceleration.

2.1.2 Establishment of similarity criteria for modeling a concrete mixture by a continuous system

The application of similarity methods to study the vibrations of a concrete mixture when modeling its continuum system uses the equation of the linear dynamic theory of elasticity, writing down one of the Lamé's equations:

$$\rho \frac{\partial^2 \omega}{\partial t^2} = (\lambda + \mu) \frac{\partial \theta}{\partial Z} + \mu \Delta \omega + Z, \quad (2.7)$$

one of the conditions on the surface:

$$\mu \left(\frac{\partial u}{\partial z} + \frac{\partial \omega}{\partial x} \right) \ell + \mu \left(\frac{\partial v}{\partial z} + \frac{\partial \omega}{\partial y} \right) m + \left(\lambda \theta + 2\mu \frac{\partial \omega}{\partial z} \right)^n = Z_v \quad (2.8)$$

and one of the expressions relating strain to stress:

$$\ell_{xy} = \frac{1}{2} \left(\frac{\partial u}{\partial y} + \frac{\partial v}{\partial x} \right) = \frac{X_y}{2\mu}, \quad (2.9)$$

bearing in mind that the continuity equation is identical for any choice of scales.

In (2.6) – (2.9) the following notation is accepted:

$$\lambda = \frac{E\sigma}{(1-2\sigma)(1+\sigma)}; \quad \mu = \frac{E}{2(1+\sigma)} \quad (2.10)$$

are Lamé's constants;

$$\theta = \frac{\partial u}{\partial x} + \frac{\partial v}{\partial y} + \frac{\partial \omega}{\partial z}$$

is volume deformation.

L, m, n – directing cosines of the angles formed between the normal \mathbf{v} to the mixture surface and the coordinate axes, respectively x, y, z ; z – the projection of the volume forces on the z axis; z_v – projection onto the z axis of the surface forces acting on the site with the normal \mathbf{v} ; ℓ_{xy}, x_y – components of the deformation and stress in the direction of the x axis along the area normal to the y axis.

Substituting for definiteness:

$$Z = \rho g + \rho \dot{\omega}_0 \quad (2.11)$$

and reducing (2.7) to dimensionless form, let's obtain a similarity criterion:

$$\frac{\lambda}{\mu} = idem \text{ or } \sigma = idem, \quad (2.12)$$

Further, taking into account (2.10), let's obtain:

$$K^2 = \frac{ET^2}{\rho L^2} = idem \text{ or } T = KL \sqrt{\frac{\rho}{E}}; \quad (2.13)$$

$$Fr = \frac{gT^2}{L} = idem \text{ or } \frac{g\rho L}{E} idem; \quad (2.14)$$

$$\frac{\ddot{\omega}_0 T^2}{L} = idem \text{ or } \frac{\dot{W}_{op} L}{E} = idem. \quad (2.15)$$

Reducing (2.8) and similar equations on the surface to a dimensionless form, let's obtain, taking into account (2.10):

$$\frac{X_v}{E} = \frac{Y_v}{E} = \frac{Z_v}{E} = idem. \quad (2.16)$$

Writing down the conditions for the generality of motion at the interface between the medium and the working body of the vibrating machine using equalities of the type (4.55), let's obtain (subscripts relate to materials from different sides of the boundary):

$$\frac{E_1}{E_2} = idem, \quad (2.17)$$

and taking into account the fact that in (2.13) the scales L and T are constant for all areas of the model:

$$\sqrt{\frac{E_1 \rho_2}{\rho_1 E_1}} = idem,$$

i. e. taking into account (2.17):

$$\frac{\rho_1}{\rho_2} = idem. \quad (2.18)$$

So, there is a fundamental possibility of creating a model that simultaneously satisfies the Froude criterion and other criteria. For this, it is necessary that the ratio of the compression wave speeds in the mixture model and the original be proportional to the root of the linear scale, i. e.

$$\frac{E}{\rho L} = idem. \quad (2.19)$$

Thus, to ensure the similarity of phenomena in the concrete mixture model, which is presented as a linearly deformed elastic body, and for a real mixture it is necessary and sufficient to ensure geometric similarity.

The energy balance of the system is considered on the basis of a discrete and continuous model of concrete mix, and the basic idea of determining the similarity criteria for concrete compaction processes is based on the assumptions that this process is accompanied by the simultaneous course of compaction, mass transfer, physicochemical transformations, can be determined as follows:

- establish the basic parameters that are components of the general expression of the energy balance, reflecting the compaction process;
- use an approach to determining criteria based on a general criterion of thermodynamic similarity, reflecting the process of formation of a mixture on the basis of general laws of change of state, regardless of the structure of the system considered.

Consideration of the energy balance by a discrete model is as follows. It is accepted that the internal energy of the chaotic motion of the particles of the mixture is generated not only due to the dissipation of the average movement, but also due to the transverse forces of the particles along the form in which the mixture is located within the allocated volume. These forces in the theory of motion of dispersed systems are usually called Magnus forces, as acting in the transverse direction when cement flows around the aggregates of a concrete mixture. There is also a decrease in internal energy due to the transition to thermal energy due to non-elastic friction of the components of the concrete mixture with each other. The energy of motion in the reduced volume V is considered as a term of the kinetic E_c and internal E_i energies:

$$E_c = \frac{1}{2} \int_V \rho V^2 dV, \quad E_i = \frac{1}{2} \int_V \rho \bar{E} dV, \quad (2.20)$$

where \bar{E} – internal energy of a unit volume.

The balance of the total energy consists of the work of external and internal forces and energy, supplied to the system:

$$\frac{d(E_c + E_i)}{dt} = \int_V (FV + \rho gh + E_M + E_d) dV, \quad (2.21)$$

where F – force acting in the system of «filler – cement paste»; E_M – Magnus energy; E_d – dissipative component of energy, in the general case also takes into account the degree of dispersion during the destruction of the structural elements of the system. The energy of the mold surface under the action of vibration creates a stress-strain state of the concrete mixture with the transfer of elementary volumes of the mixture from an uncompressed state to another, more densified state. That is, mass transfer processes occur that cause energy dissipation due to the movement of the components of the mixture and, as the final result, its compaction.

The general energy balance (2.21) is based on the equations of a continuous medium, which moves under the influence of a pallet of the form in which the concrete mixture is located.

The motion of a continuous medium is described by a mathematical model:

$$\frac{d\bar{V}}{dt} = -\frac{1}{\rho} \nabla \sigma + \bar{f}, \quad (2.22)$$

where

$$\frac{d\bar{V}}{dt} = \frac{\partial \bar{V}}{\partial t} + (\bar{V} \nabla) \bar{V}$$

is total time derivative t ; $\bar{V} = \{V_r, V_\varphi, V_z\}$ – speed vector of the elementary volume of the mixture; V_r, V_φ, V_z – radial, tangential and axial components of the flow speed vector in the r and z directions; ρ – density of the mixture; ∇ – Hamilton differential operator; σ – stress tensor; \bar{f} – vector referred to a unit of mass.

For stationary motion, in a first approximation corresponds to the movement of concrete mixture, it is possible to accept:

$$\frac{\partial \bar{V}}{\partial t} = 0,$$

and model (2.16) is represented by the Navier-Stokes differential equation.

To describe the motion of a viscous medium, which is a concrete mixture, model (2.22) is represented by the Navier-Stokes differential equation system [6], the solution of which is reduced to determining the speed of the medium and pressure.

The energy criterion for modeling compaction processes is determined from the ratio of energies:

$$\frac{TdS}{dE} - \left(\frac{\partial u}{\partial t}\right) d\left(\frac{1}{\rho}\right) = idem, \quad (2.23)$$

where TdS – energy (entropy) supplied by the working body; dE – total energy of the system.

The equations of balance of the total energy can be represented from the position of consideration of a continuous medium with components of its stress-strain state:

$$dE = dE_c + dE_p + dE_e, \quad (2.24)$$

where dE_c , dE_p , dE_e – kinetic, potential, and elastic strain energies, respectively.

Considering the energy E_e within the elastic deformation in accordance with the dependence $\sigma = E\varepsilon$, where E – the elastic modulus, and ε – the relative deformation, the expression for energy can be represented in the form [7]:

$$dE_e = 0.5\sigma^2 \Delta V / E, \quad (2.25)$$

where ΔV – elementary volume of the mixture.

Other components of the energy balance of the studied system are evaluated by determining similarity criteria and their parameters.

Application of the criteria (2.18) broadens the understanding of the process of concrete mixture formation. An analysis of the components of these criteria indicates that for a generalized criterion, it is possible to use the ratio of criterion K_6 (Reynolds criterion) and criterion K_5 (Froude criterion):

$$K_{R.F.} = \rho g R / \mu \omega, \quad (2.26)$$

which by physical nature determines the ratio of mass forces and friction forces.

2.2 Investigation of the interaction of aggregate particles with a technical system of vibration exposure

2.2.1 Background and assumptions

In the studies, the assumption is made that when vibration affects the concrete mixture, the friction in the places of contact of the particles decreases, and under the influence of gravitational forces, the particles tend to a position corresponding to a denser packing. It is assumed that this phenomenon is associated with a purely mechanical effect of reducing the friction of the granular material.

In determining the process of particle interaction, it is assumed that dry friction forces prevail in the system, and viscoelastic forces prevail at the final stage.

2.2.2 Investigation of the interaction process of particles of aggregate concrete mixture

The effect of vibration on the fraction with dry friction can be estimated by the effective coefficient of friction, which is determined from the known relations [8, 9]:

$$f_{ef} = \frac{F_{\min}}{N} = f_1 \sqrt{1 - \frac{(F_0 \sin \omega t)^2}{f_1 N}}, \quad (2.27)$$

$$f_{ef} = f_1(N - F_0 \sin \omega t), \quad (2.28)$$

where f_1 is the coefficient of dry frictional rest; F_{\min} – force, which sets the particle in motion from a state of rest; N – normal reaction; F_0 – disturbing force.

Expression (2.27) can be used in cases where the perturbing force is perpendicular to the normal reaction, and (2.28) when parallel to the normal reaction N . An analysis of dependences (2.27), (2.28) shows that the effective coefficient of friction in all cases, with an increase in amplitude, decreases to zero.

When exposed to the bulk material by vibration, the material comes into a state of vibrational shock, characterized by a decrease in friction between the particles and their slippage relative to each other, which contributes to a denser packing. This situation is valid in cases where the acceleration of vibrations of the vibrational technical system on which the particles are located does not exceed 1 g.

With an increase in acceleration, a transition of the medium from the state of vibration excitation to vibration boiling is observed [8].

In the state of the vibration boiling, the particles periodically break away from each other and from the vibrating surface. As a result, the volume of the layer increases, the internal friction in the system is significantly reduced, and mixing of the material begins. The influence of external vibration parameters on the transition of the system to the vibration boiling state depends on the material of the particles, in particular, their density.

The equations of motion of a particle, an oscillating medium, in general form can be written:

$$m\ddot{x}_p = m_m \left(\frac{\rho}{\rho_0} - 1 \right) (g - \ddot{x}_m) + F_{df}, \quad (2.29)$$

where m – mass of the particle; m_m – mass of the medium in a volume equal to the volume of the particle; ρ – particle density; ρ_0 – density of the medium, particle acceleration relative to the medium; \ddot{x}_m – acceleration of the medium at a point coinciding with the center of gravity of the particle; g – acceleration of gravity; F_{df} – force with which the medium acts on the particle.

For the case of dry friction F_m , the force will be equal to:

$$F_m = -m_{at}\ddot{x}_p + F(\dot{x}), \quad (2.30)$$

where m_{at} – attached mass; $F(\dot{x})$ – resistance force to the relative motion of the particle.

$$F(\dot{x}) = 0 \text{ at } \dot{x} = 0.$$

When equality (2.30) is taken into account, the equation of motion of the particle will take the following form:

$$(m + m_a)\ddot{x}_p = m_{em} \left(\frac{\rho}{\rho_0} - 1 \right) (g - \ddot{x}_m) + F_{df}. \quad (2.31)$$

Let's consider the case when the particles of the medium move along circular paths lying in the horizontal plane (Fig. 2.1) [8]. The projections on the $OXYZ$ axis of the absolute speed of the unperturbed motion of the medium near the particle are given by the following relationships:

$$\dot{x}_{mx} = -A\omega \sin(\omega t + \alpha); \quad \dot{x}_{my} = A\omega \cos(\omega t + \alpha); \quad x_m = 0,$$

where A – amplitude of the circular trajectory of the oscillations; ω – oscillation frequency; α – initial phase.

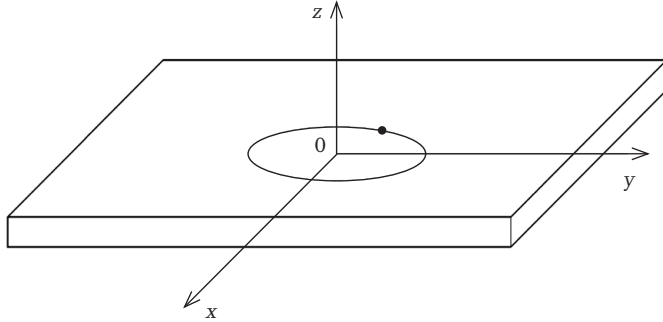


Fig. 2.1 Particle motion pattern

Introducing the concept F_c — the module of the resistance force when moving in a horizontal position; F_p — the modulus of the resistance force in relative motion in the vertical direction, let's obtain the equation of motion of the particle in projections on the moving coordinate axes.

Then, by direct substitution, when the condition is satisfied, let's obtain:

$$\frac{F_p}{m_m g} > \left| \frac{\rho}{\rho_0} - 1 \right| \geq \frac{1}{\sqrt{\left(\frac{m_m A \omega^2}{F_c} \right)^2 + \left(\frac{m_m g}{F_o} \right)^2}}. \quad (2.32)$$

Let's make sure that the system of linear equations (2.32) admits a solution of the type:

$$\begin{aligned} \dot{x}_{x,o} &= R\omega \cos(\omega t + \beta); \quad \dot{x}_{y,o} = R\omega \sin(\omega t + \beta); \\ \dot{x}_{z,o} &= \frac{\delta}{\sqrt{1 - \delta^2}} R\omega, \end{aligned} \quad (2.33)$$

where

$$\begin{aligned} R &= A \sqrt{\left[\frac{m_m}{m + m_a} \left(\frac{\rho}{\rho_0} - 1 \right) \right]^2 - \left[\frac{F_c}{(m + m_a) A \omega^2} \right]^2 (1 - \delta)^2}; \\ \delta &= \frac{m_m \left(\frac{\rho}{\rho_0} - 1 \right) g}{F_e}. \end{aligned}$$

The solution of the equation corresponds to the movement of a particle along a helical line with a vertical axis, which has a radius R and a step:

$$h = \dot{x}_{ez0} \frac{2\pi}{\omega} = \frac{2\pi\delta}{\sqrt{1-\delta^2}} R.$$

From the obtained relations it follows that when conditions (2.33) are fulfilled, particles with a density $\rho > \rho_0$ are immersed in the medium, and the particles $\rho < \rho_0$ are float. When the results are disseminated to concrete mixtures, the phenomenon of separation is explained, when, under prolonged exposure to vibration, settling of coarse aggregate particles is observed.

The vertical component of the particle speed is equal to:

$$\begin{aligned} \dot{x}_{pz.o} &= \frac{\delta}{\sqrt{1-\delta^2}} R\omega = \\ &= \frac{m_m \left(\frac{\rho}{\rho_0} - 1 \right) g}{F_e} R\omega \cdot \sqrt{\left[\frac{m_m \left(\frac{\rho}{\rho_0} - 1 \right)}{(m + m_a)\sqrt{1-\delta^2}} \right]^2 - \left[\frac{F_c}{(m + m_a)A\omega^2} \right]^2}. \end{aligned} \quad (2.34)$$

Comparing (2.34) with the well-known dependence of the free fall rate of a spherical particle in a viscous fluid at low numbers R_e (according to Stokes), let's obtain:

$$\dot{x}_{pz0} = \frac{m_m \left(\frac{\rho}{\rho_0} - 1 \right) g}{3\pi\eta^* d}, \quad (2.35)$$

where η^* – viscosity coefficient of the medium; d – particle diameter.

Let's find the effective coefficient of viscosity of the medium:

$$\eta^* = \frac{F_0}{3\pi d A \omega} \sqrt{\left[\frac{m_m \left(\frac{\rho}{\rho_0} - 1 \right)}{(m + m_a)\sqrt{1-\delta^2}} \right]^2 - \left[\frac{F_c}{(m + m_a)A\omega^2} \right]^2}. \quad (2.36)$$

This dependence explains the conditions for the imaginary rarefaction of a granular medium under the action of vibrations, which is a purely mechanical phenomenon. When the vibration ceases, the effect of «dilution» instantly ceases.

For the case of vertically directed oscillations, the particle immersion rate can be determined by the following dependence [8]:

$$\dot{x}_{pz0} = \frac{m_m \left(\frac{\rho}{\rho_0} - 1 \right) A \omega}{(m + m_a) \pi} f(\lambda, \mu),$$

where $f(\lambda, \mu)$ – function, taking into account the ratio of dimensionless coefficients λ and μ .

$$\lambda = \frac{F_e}{m_m \left(\frac{\rho}{\rho_0} - 1 \right) A \omega^2}; \quad \mu = \frac{g}{A \omega^2}.$$

Using equality (2.35), it is easy to determine the effective viscosity coefficient for regimes with vertically directed oscillations:

$$\eta^* = \frac{(m + m_a)g}{3dA\omega^2} \cdot \frac{1}{f(\lambda, \mu)}, \quad (2.37)$$

or, when presented m and m_e through particle diameter and density ρ :

$$\eta^* = \frac{\pi d^2 \rho g}{12A\omega^2} \cdot \frac{1}{f(\lambda, \mu)}. \quad (2.38)$$

It follows that with an increase in the diameter of the particles $A\omega^2 = \text{const}$, the apparent viscosity of the medium increases. The second consequence is that particles of different diameters oscillate with a speed gradient and a certain phase shift. This position is well confirmed by experimental data.

The decrease in the friction forces between particles is mainly of Coulomb origin, it is advisable to obtain by the action of large amplitudes of oscillations at a sufficiently low frequency, since the use of high frequencies due to their rapid attenuation is less rational. Such modes, as experience has shown, give high efficiency compaction of concrete mixtures at the initial stage of formation [10].

With the formation of a coating layer of the solution between the coarse aggregate particles and the end of the period of destruction of the concrete structure, there is a partial transformation of dry to viscous friction. Under these conditions, the behavior of the aggregate particles differs from the previously considered.

Let's consider the motion of a solid particle in a medium with viscous resistance. It is known that on a spherical particle in a wave field of a viscous medium, the force of internal friction and resistance to vibrational movements equal to [11]:

$$F = 6\pi\eta r \left(1 + r \sqrt{\frac{\rho\omega}{2\eta}} \right) \dot{x}, \quad (2.39)$$

where η – vibration viscosity of the medium; r – particle radius; ρ – density of the medium; ω – oscillation frequency; \dot{x} – speed of oscillations.

Then the equation of motion of the particle can be written in the following form:

$$\left[j\omega(m_m - m_a) - 6\pi\eta r \left(1 + r \sqrt{\frac{\rho\omega}{2\eta}} \right) \right] (\dot{x}_m - \dot{x}_p) = j\omega(m_m - m_a)\dot{x}_p, \quad (2.40)$$

where, as in the consideration of equation (2.31), m_m – mass of the medium in a volume equal to the volume of the particle; m_a – attached mass of the particle; \dot{x}_m, \dot{x}_p – speed of the medium and particles.

Solving the equation, let's obtain an expression for the ratio of particle speed and medium speed or the ratio of their amplitudes:

$$\frac{\dot{u}_p}{\dot{u}_e} = \frac{A_p}{A_{dt}} = \frac{1 + \frac{j}{\Omega} \left(1 + r \sqrt{\frac{\rho\omega}{2\eta}} \right)}{\frac{m + m_a}{(m_e + m_a)} + \frac{j}{\Omega} \left(1 + r \sqrt{\frac{\rho\omega}{2\eta}} \right)}, \quad (2.41)$$

where

$$\Omega = \frac{f}{fg} = \frac{f(m_m + m_a)}{3\eta r} = \frac{\omega(m_m + m_a)}{6\pi\eta r},$$

where f – oscillation frequency; fg – characteristic frequency.

To determine the ratio of the amplitudes of particle oscillations through the parameters of the medium, let's define the modulus of the value (2.41).

Let's introduce the notation:

$$\frac{m + m_e}{m_m + m_e} = \alpha,$$

$$\frac{\Omega}{\left(1+r\sqrt{\frac{\rho\omega}{2\eta}}\right)} = \beta.$$

Then the ratio of amplitudes can be expressed as:

$$\begin{aligned} \frac{A_p}{A_m} &= \frac{\left|1 + \frac{j}{\beta}\right|}{\left|\alpha + \frac{j}{\beta}\right|} = \frac{1}{\alpha^2\beta^2 + 1} \sqrt{(\alpha\beta^2 + 1)^2 + (\alpha\beta - \beta^2)^2} = \\ &= \frac{1}{\alpha^2 + \frac{1}{\beta^2}} \sqrt{\alpha^2 + \frac{\alpha^2}{\beta^2} + \frac{1}{\beta^2} + \frac{1}{\beta^4}}. \end{aligned} \quad (2.42)$$

Let's consider the case when $\Omega \gg 1$, that is, under the condition that the main frequency of the oscillations of the medium is higher than the characteristic one. For small r ($\beta \gg 1$) let's obtain have:

$$\frac{A}{A_m} \approx \frac{1}{\alpha^2} \sqrt{\alpha^2} \approx \frac{1}{\alpha} \approx \frac{m_m + m_e}{m + m_e}. \quad (2.43)$$

In addition to the attached mass $m_a = m/2$, let's obtain:

$$\frac{A_p}{A_m} \approx \frac{\rho + \frac{1}{2}\rho}{\rho_0 + \frac{1}{2}\rho}. \quad (2.44)$$

Dependence (2.44) shows that in the case of approaching the density of the medium and the particle, the ratio of the amplitudes of the oscillations moves to unity. If the particle density is less than the density of the medium ($\rho < \rho_0$), then the amplitude of the oscillations of the particles will be greater than the medium, and vice versa.

The resulting ratio requires experimental evaluation.

According to the work, it follows that the relative vibrations are denser than the medium, the particles lag behind in phase from the corresponding fluctuations of the flow in the range of $90 - 180^\circ$. If the fraction has a density lower than the medium, then its relative oscillations are ahead of the fluctuations of the flow, and the phase shift lies in the range $0 - 90^\circ$.

The phase shift between the oscillations of the particle and the medium can be obtained using the following relationship:

$$\varphi = \operatorname{arctg} \frac{9}{4} \left(\frac{1+r \sqrt{\frac{\rho\omega}{2\eta}}}{r^2 \frac{\rho\omega}{2\eta} \cdot \frac{\rho}{\rho_0} + \frac{1}{2} + \frac{9}{4} r \sqrt{\frac{2\eta}{\rho\omega}}} \right). \quad (2.45)$$

Dependence (2.45) allows one to analytically calculate the particle vibration parameters for a wide class of concrete mixtures. Thus, taking a particular model according to established criteria and theoretical studies of the interaction of aggregate particles with a technical system of vibration exposure, it is possible to determine the parameters of the vibrational compaction process that ensure the maximum value of the density of the mixture under conditions of minimal energy consumption.

Chapter 3

Research of change in the state of dispersed media and technical systems under the action of power loads

3.1 Intensification of the energy impact on the working medium in the conditions of shock and vibration shock destruction of soils

The intensification of the destruction of the working medium due to high cutting speeds has a number of advantages, which include a relatively simple working movement of the cutting elements, a fairly simple drive of the machines, and the implementation of a dynamic load on the working medium.

The interaction of cutting elements with the soil under conditions of high-speed cutting occurs with variable geometric, kinematic and power parameters. Moreover, this interaction has a spatial character, where the interaction characteristics are quantitatively and qualitatively variable in different parts of the stress-strain state of the soil in the cutting zone. That is, the response of the working medium to the load is differentiated in space and time.

At the moment after a large panning with a blocked rectangular cutting, the cutting element is in contact with the undestroyed working medium along the $ABCD$ plane (Fig. 3.1). In this case, with further movement at the initial moment along the $ABCD$ plane, the processes of compression, tension, shear and internal friction, as well as external friction of the soil along the front edge of the knife, occur in the soil. The medium is cut along the lateral lines AB and CD (on the front and side edges) and the lower line AD (cutting edge).

In addition to soil properties, the nature of the stress-strain state is influenced by both geometrical and kinematic parameters, as well as power and energy parameters, in particular, cutting depth h , cutting angle δ , interaction speed of cutting elements V_{cut} and the magnitude of specific energy actions of the working body on the soil. At the initial moment, stress on the BC line will be zero, and on the AD line the maximum, despite the fact

that the movement of the cutting element in the horizontal direction is the same for the particles of the working medium located on the BC line and the AD line, and the particle displacement on these lines is generally identical in modulus and direction, but the conditions of the particles located on the BC line and the AD line will be different.

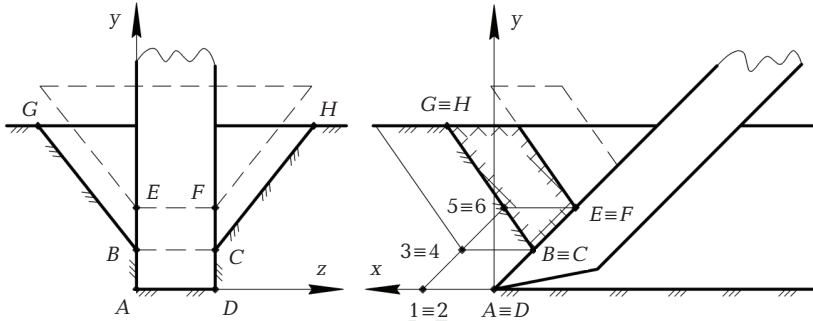


Fig. 3.1 Differentiated scheme for determining the power and energy parameters when cutting soils

It should be noted that the interaction of bodies or particles with one another, which leads to a change in the state of their motion, occurs over one or another field discretely distributed in space. Currently, depending on the particles that make up the body, these fields are divided into four types of fundamental interactions. These interactions (in order of increasing intensity of interaction) are gravitational interaction, weak interaction, electromagnetic interaction, strong interaction. The intensity of interaction is determined by the coupling constants. Interaction only through physical fields occurs at both the micro and macro levels.

For soil destruction, the interaction between soil particles occurs due to the electromagnetic and gravitational fundamental interactions, which have such interaction constants: e – elementary electric charge (electromagnetic interaction constant) and G – gravitational constant. The strength of the interaction between soil particles depends on the strength of the physical field:

$$F = EW, \tag{3.1}$$

where E – intensity of the physical field; W – value of the field of the soluble parameter.

For the gravitational field $E = G_g \approx g$. Here G_g – the gravitational field strength is equal to the force acting on the unit field of the soluble parameter – mass; g – acceleration of gravity. An electromagnetic field

is characterized by a vector of electric field strength E and magnetic induction B , which determine the forces acting from the field side on stationary and moving charged particles. The electromagnetic field strength corresponds to the principle of superposition, according to which the total field strength at a point is equal to the geometric sum of the fields created by individual charged particles. In addition, the force of interaction between particles is inversely proportional to the square of the distance between them.

Thus, the intensity of interaction between particles of the working medium on the AD line will be much greater than on the BC line. For the same reason, the highest intensity of interaction between particles of the working medium will be at points A and D .

A common characteristic of the interaction is potential energy. This binding energy of a system of particles or bodies is equal to the work that needs to be spent to divide this system into the components that make up it and remove these components from each other at such distances that the interaction between them could be neglected. In the case of macrosystems, which are represented in the working processes of soil technology by soils, the binding energy is equal to the work expended on the destruction of the working media. In general, work on soil destruction is equal to the binding energy between the parts of the destroyed soil and the energy spent on residual deformations in the destroyed soil.

When moving the cutting element at a distance equal to a single large cleavage and is determined by the formula:

$$l_{cl} = (hk_h - a)(ctg\delta + ctg\theta), \quad (3.2)$$

where h – depth of cut by the cutting element; k_h – coefficient of contact of the tooth with the soil, depending on the angle of cutting δ ; $a = h(1 - k_{side})$ – length of side openings; y' – depth coefficient of the part of the opening expands; $\theta = \pi/4 - \rho_i/2$ – angle between the cutting path and the preferred direction of movement of the pieces of soil chips; angle of internal friction.

Soil cutting occurs along two lateral surfaces $135B$ and $246CD$. These surfaces are similar to each other. They consist of two parallelograms $P1$ (points $13BA$) and $P2$ (points $24CD$) and two triangles $T1$ (points $35B$) and $T2$ (points $46C$).

The areas of parallelograms will be equal $S_{P_1} = S_{P_2} = al_{cl}$.

The area of the triangles will be equal $S_{T_1} = S_{T_2} = 0.5l_{cl}(hk_h - a)$.

If the contact area of the cutting element with the soil in the area where the cut occurs during the cutting process in the part of the opening, the parallelogram is limited unchanged, then in the part of the opening, limited by triangles it changes from zero to $S_{KT_1} = \Delta b35$ and $S_{KT_2} = \Delta l46$. Here, Δb – the width of the destroyed soil when cut by side edges by cutting elements.

Then the contact area of the cutting element with the soil in the zone of parallelograms will be $S_{KP_1} = \Delta b13 = \Delta bAB$ and $S_{KP_2} = \Delta b24 = \Delta bCD$.

The contact area of the cutting element with the soil when cutting along the line AD will be equal.

Let's write the equation of work for all sections of the cross-section of the opening spent on cleaving a single large cleavage.

Cutting process with a cutting edge (line AD):

$$A_{AD} = \int_0^{l_{cl}} F_{\tau AD}(x) dx, \quad (3.3)$$

where $F_{\tau AD}(x)$ – function of the dependence of the tangent cutting force acting on the cutting edge (line AD) on the movement of the cutting element in the soil:

$$A_{AD} = \phi \Delta b \int \int_{G_1} \sigma_1(x, z) dx dz, \quad (3.4)$$

where ϕ – coefficient taking into account the cutting angle; $\sigma_1(x, z)$ – dependence of the change in stress normal to the speed of movement of the cutting element in the soil along the width of the cutting element (along the z axis) for a given position of the cutting element in the face (x coordinate); G_1 – region where a continuous function of the dependence of normal stresses σ on the variables x and z for the cutting edges (line AD).

In addition to the process of cutting the soil with a cutting edge along the line AD , there is a process of external friction of the edge of the cutting element relative to the soil along the bottom of the opening.

External friction is characterized by two qualitatively different processes, namely, energy losses on the one hand to overcome molecular bonds and, on the other, to shape change of the surface state of the material of bodies interacting.

It should be noted that due to the significant unevenness of the surfaces in contact, contact between these surfaces occurs only at individual «touch points» that are concentrated on the tops of the protrusions of the surfaces.

The total coefficient of external friction is determined by the formula [12]:

$$f = f_{mol} + f_{mech} = \frac{\tau_0}{\rho_s} + \beta + k \alpha_h \sqrt{\frac{h}{R}}, \quad (3.5)$$

where f_{mol} – the coefficient of friction characterizing the occurrence of friction during the molecular interaction of surfaces in contact; f_{mech} – the same thing when shaping these surfaces; τ_0 – shear strength of a single «point» of contact (friction coupling) in the absence of compressive load; β – friction bond strengthening coefficient; ρ_s – actual pressure at the

point of contact; k – coefficient depending on the location of the irregularities in height; R – radius of a single roughness modeled by a spherical segment; h – immersion depth of a single roughness; α_h – hysteresis loss coefficient.

Hence, the friction force for the cutting edge is determined by the formula:

$$F_{TAD} = fF_{\tau AD} \operatorname{ctg}(\delta + \mu), \quad (3.6)$$

where δ – cutting angle; μ – angle of external friction is determined by the formula:

$$\mu = \operatorname{arctg}(f), \quad (3.7)$$

Slice work of the part AB of front side edge:

$$A_{AB} = \int_0^{l_{cl}} F_{\tau AB}(x) dx, \quad (3.8)$$

where $F_{\tau AB}(x)$ – function of the dependence of the tangential cutting force acting on part AB of the front side edge on the movement of the cutting element in the soil,

$$A_{AB} = \phi \Delta b \iint_{G_2} \sigma_2(x, y) dx dy, \quad (3.9)$$

where $\sigma_2(x, y)$ – dependence of the change in stress normal to the direction of the speed of movement of the cutting element in the soil for part AB of the front side edge along the y axis; S – region where the continuous function of the dependence of normal stresses σ on the variables x and y is given for part AB of the front side edge (line AB).

Friction force for part AB of the front side edge:

$$F_{TAB} = \xi f F_{\tau AB}, \quad (3.10)$$

where ξ – lateral pressure coefficient.

The lateral pressure coefficient characterizes the ratio of the increase in lateral pressure to the increase in compressive pressure, is determined by the formula:

$$\xi = \frac{\nu}{1 - \nu}, \quad (3.11)$$

where ν – lateral expansion coefficient of the soil (Poisson's ratio).

Operation of the shear process by part of the BE of the front side edge:

$$A_{BE} = \int_0^{l_{cl}} F_{\tau BE}(x) dx, \quad (3.12)$$

where $F_{\tau BE}(x)$ – function of the dependence of the tangential cutting force acting on part BE of the front side edge on the movement of the cutting element in the soil.

$$A_{BE} = \phi \Delta b \int \int_{G_3} \sigma_3(x, y) dx dy, \quad (3.13)$$

where $\sigma_3(x, y)$ – dependence of the change in stress normal to the direction of the speed of movement of the cutting element in the soil for part BE of the front side edge on the x and y coordinates. If the area of contact with the soil during its destruction by the cutting edge AD and part of the front side edge AB is constant:

$$S_{AD} = \Delta b l_{AD}; \quad S_{AB} = \Delta b l_{AB}, \quad (3.14)$$

where l_{AD} and h_i , respectively, the lengths of the segments AD and AB , the part of the side edge above the segment AB destroys the soil with an area from 0 to

$$S_{BE} = \Delta b l_{BE}. \quad (3.15)$$

Friction force for the BE part of the front side edge:

$$F_{TBE} = \xi f F_{\tau BE}. \quad (3.16)$$

Soil destruction work by the front face of the cutting element:

$$A_{ABEFCD} = \int_0^{l_{cl}} F_{\tau ABEFCD}(x) dx, \quad (3.17)$$

where $F_{\tau ABEFCD}(x)$ – function of the dependence of the tangent force of deformation (destruction) of the soil by the front face of the cutting element on the movement of this element in the soil.

$$A_{ABEFCD} = \phi \iiint_V \sigma_4(x, y, z) dx dy dz, \quad (3.18)$$

where $\sigma_4(x, y, z)$ – dependence of the change in stress normal to the direction of the speed of movement of the cutting element in the soil for the front face on the x , y and z coordinates; V – the volume where the continuous function of the dependence of normal stresses σ on the variables x , y , z for the front face $ABEFCD$ is given.

During the formation of a large cleavage and to its cleavage, the contact area of the front face with the soil varies from minimum S_{ABCD} to maximum S_{AEFD} . Thus, deformation and destruction by cutting elements of the soil under cutting conditions is inherent in the differentiation of physical processes in space and time with different energy values necessary for the destruction of soils in different zones. Therefore, the organization of the effective destruction of the working medium consists in the direction to different parts of the working area of the corresponding energy flows of the required magnitude with specific specific parameters.

The tangential average forces arising in different parts of the contact zone of the cutting element with the working medium without taking into account the friction forces will be determined from the formulas:

– for cutting edge:

$$F_{\tau AD} = \frac{\phi \Delta b \iint_{G_1} \sigma_1(x, z) dx dz}{l_{cl}}; \quad (3.19)$$

– for side edges:

$$F_{\tau ABE} = \frac{2}{l_{cl}} \left(\phi \Delta b \left(\iint_{G_2} \sigma_2(x, y) dx dy + \iint_{G_3} \sigma_3(x, y) dx dy \right) \right); \quad (3.20)$$

– for the front face:

$$F_{\tau ABEFCD} = \frac{\phi \iiint_V \sigma_4(x, y, z) dx dy dz}{l_{cl}}. \quad (3.21)$$

Integration by numerical methods in the above formulas is performed in accordance with the nature of the dependences of normal stresses in the cutting zone (Fig. 3.2 – 3.4, as well as Fig. 3.5 [13]).

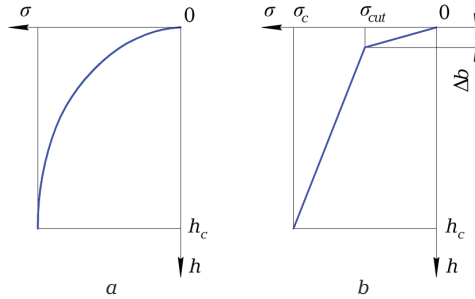


Fig. 3.2 Dependence of pressures on the front face of the cutting element, normal to the direction of cutting speed, on the depth of cut for loosely bound soils: *a* – nature of the dependence $\sigma = f(h)$; *b* – approximation of dependence $P = f(h)$

Here h_c – depth of cut by the cutting element; σ_c – stress, determined by the maximum granularity of dispersed media.

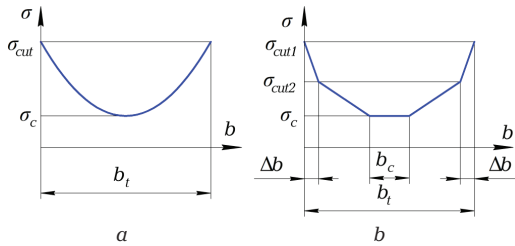


Fig. 3.3 Pressure distribution on the front face of the cutting element along the width of the tooth $b_t \sigma(b)$: *a* – nature of the dependence $\sigma(b)$; *b* – approximation of dependence $\sigma(b)$

Here σ_{cut1} , σ_{cut2} – distributions in the cutting zone; σ_c – value of the minimum stress in the central zone.

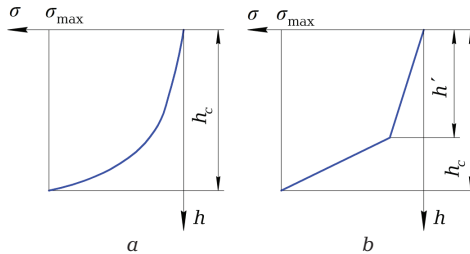


Fig. 3.4 The dependence of normal stresses in the soil in contact with the front face of the cutting element when cutting cohesive plastic soils: *a* – nature of the dependence $\sigma = f(h)$; *b* – approximation of dependence $\sigma = f(h)$

Here h_c – depth of cut; h' – conditional depth; σ_{\max} – maximum stresses at points A and D.

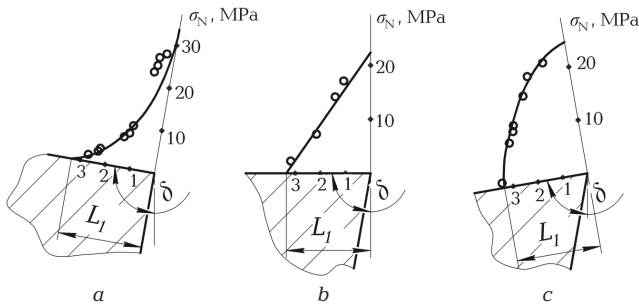


Fig. 3.5 The influence of the cutting angle on the distribution of normal stresses on the front face of the tool (cutting lead) [13]:

$a - \delta = 100^\circ$; $b - \delta = 90^\circ$; $c - \delta = 80^\circ$

3.2 The general movement of the working bodies of soil-grinding machines and working media as a single synergetic system

The movement of destructive elements of earth-moving machines is characterized by geometric kinematic, power and energy parameters. This movement occurs both in relation to the immovable working medium, and in relation to the fractions of the destroyed soil, which move at certain trajectories with certain speeds and accelerations in the face. Even in the case when the destructive elements move relative to an immovable soil mass in contact with it, the soil characteristics depend on spatial coordinates, as well as on the speed of interaction of the cutting elements with the soil. In addition, physical processes occurring in the contact zone of the working bodies with the working medium, which have certain differences and features depending on the spatial coordinates of the soil destruction zone, also belong to the parameters of joint motion. In each area of the destruction zone, self-organizing processes take place, which in general terms as subsystems form a self-organizing system of the process of destruction of working media by the working bodies of technological grounding systems. In the fracture zone, processes of deformation of the working media, processes of occurrence and propagation of waves of deformation, processes of destruction, processes of movement of cutting elements and destroyed soil, processes of impact collision of soil particles between themselves and cutting elements, secondary dispersion processes and friction processes occur.

Taking into account the complex synergistic nature of the interaction of working bodies with the working medium requires a deep analysis of the

processes occurring in the fracture zone, both in space and in time. The structures of destructive elements and their operating modes must take into account the features of specific individual sections of their contact zone with the working media and processes that occur there so that they are most consistent with the processes of self-organization of movement in these areas.

An important part of the contact zone between the interaction of the cutting elements and the working medium is the limiting zone along some part of the perimeter of the cutting element consists of a cutting edge and a part of the front side ribs. On this site, in general terms, the cutting occurs with the cutting edge and the front side ribs of the soil and their friction against the soil. In this section, the fracture conditions are the most difficult, which is expressed in the largest specific forces of soil resistance to fracture, as well as in the intensive abrasive wear of the corresponding parts of the cutting elements. Thus, in this area, three separate processes can be distinguished: destruction of the working medium, its cutting and intensive friction processes, lead to significant abrasive wear of the cutting elements, therefore, to work in this area, a part of the cutting element performs this work must have an appropriate design and properties. To perform soil cutting and minimize wear of the cutting element, it is necessary to apply in this zone for it, firstly, materials with high cutting properties, and secondly, high wear resistance. Abrasive materials having a Mohs hardness of nine, ten units correspond to this condition. These include: silicon carbide (carborundum – black and green), corundum, electrocorundum, boron carbide, whose hardness on the Mohs scale is nine, as well as super hard materials with a hardness of more than nine. These include natural and synthetic diamonds, as well as artificial cubic boron nitride (CBN). To separate the processes of destruction, cutting and friction, the design of the cutting element is formed according to the differential principle [14]. The design of this cutting (developed) element is adapted (differentiated) to various conditions for its interaction with the soil. In Fig. 3.6 a fragment of the lateral surface of the working body with the developed elements of differential design is presented, where ω and V_f are the angular rotation speed and feed rate of the working body, δ is the optimal cutting angle to the tangent to the cutting path;

The element being developed consists of an abrasive, for example, diamond element with a frontal surface $ABCDE$, in the frontal part of which a plate 1 is attached with the frontal surface also $ABCDE$, which overlaps the frontal surface of the diamond element. The diamond element consists of a diamond-free layer 2 with a frontal surface of $AdefE$ and a diamondiferous layer 3 with a frontal surface of $dBCDfe$, which, in turn, consists of diamond grains and a bundle. Plate 1 consists of a working part 4 with a frontal surface $ABCDEg$ and a non-working part 5 with a frontal surface AgE . The developed element is attached to the diamond-free part 2 and non-working part 5 to the body 6 of the working body. In general, the developed element

is as follows. As a result of the working movement with a cutting depth smaller than the grain size of diamond grains, the developed element cuts the material with diamond grains located on the BCD line. With an increase in the productivity of the development of materials, the cutting depth of the developed element increases, and, accordingly, the depth of contact h of the developed element with the working medium increases. In this case, the developed element is in contact with the developed material on the surface of $aBCDcb$. In this case, the plate 1 is in contact with the working medium on the surface of $aBCDcb$ and destroys it within this surface. The plate 1 is made of a wear-resistant material and of such a shape, optimally adapted to macrocracking, therefore, the destruction and movement of the destroyed working medium along the plate occurs with the least energy consumption. Due to the fact that the plate 1 with its frontal surface $ABCDE$ overlaps the frontal surface of the $ABCDE$ diamond element, the diamond grains of the frontal surface of $ABCDE$ do not come into contact with the material being developed and are removed from the process of fracturing the working medium along this surface, because the fracture by the diamond segment over the surface with a height is more granularity of diamond grains unproductive.

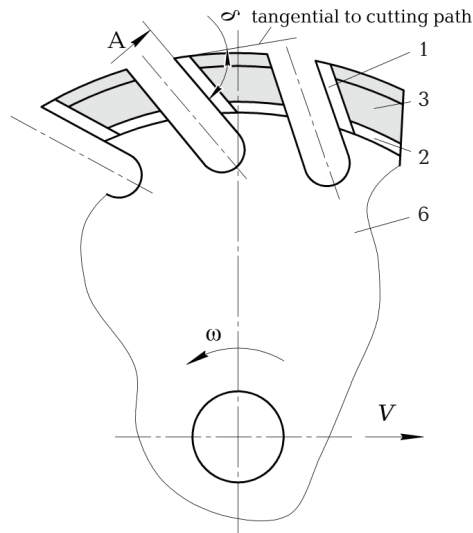


Fig. 3.6 A fragment of the lateral surface of the working body with the developed elements of differential design

In Fig. 3.7 developed element of differential construction (type A on the frontal part of the developed element), where h is the depth of contact of the developed element with the working medium.

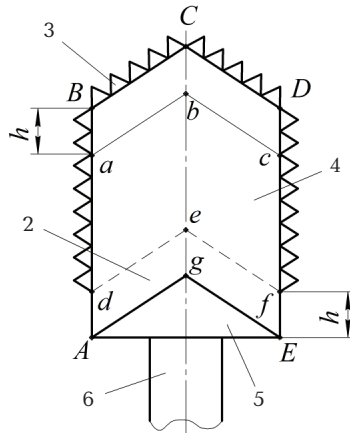


Fig. 3.7 Developed element of differential design

Since the diamond grains of the frontal surface will enter the working medium and contacts will be in contact with it, which will wear out intensively, leading to the loss of diamond grains and the formation of wear sites, further increasing the energy consumption of cutting. In addition, diamond grains of the frontal surface will additionally unproductively disperse the material being developed and create significant resistance when moving the destroyed material along the frontal surface of the element being developed, which also leads to significant increases in the energy consumption of material development and diamond wear.

Cutting of the working medium by the developed element along the $aBCDc$ line is performed by diamond grains, and plate 1 does not take part in the cutting process, therefore, dulling of the plate along the $aBCDc$ line does not occur. Thus, diamond grains perform microcuts, and plate 1 – macrocutting. The wear of the plate 1 in the operation process takes place in the form of its shortening while maintaining the practically design shape of the outline of the element being developed, that is, there are no areas for wear or rounding. Due to the fact that the entire developed element takes up the forces of resistance of the working medium to destruction, the plate 1 has a small thickness, which is determined only by the value of its abrasive wear on the frontal part for the full service life of the developed element. When the element being developed has worked out its resource (the diamond-bearing layer of the diamond element is completely worn out), its shape is determined by the frontal surface of $AdefE$. From this it follows that the frontal surface of the inoperative part 5 of the plate 1 at the time of the development of the developed element does not come into contact with the working medium and can be made of cheaper material with reduced physical and mechanical characteristics.

The geometric, physical and mechanical and all parameters that are used in the design are coordinated in such a way that they take into account the natural nature of the wear of all elements of the developed element for specific operating conditions of the working bodies of material-grinding machines.

In the process of destruction of the working medium by the plate 1, the cutting angle plays an important role in reducing the energy intensity, therefore, the element being developed is performed in such a way that the plate 1 is oriented with its frontal (front) face at the optimal cutting angle δ to the tangent to the cutting path.

Due to the fact that the main volume of the material is destroyed by the plate 1, the volume of the material is destroyed by diamond grains is significantly reduced. This greatly increases the resource of the diamond element, and due to the fact that diamond grains perform the cutting, the resource of the plate 1, in turn, also significantly increases, that is, there is a synergistic interaction of the two components of the element being developed with a positive effect on each other.

Instead of fastening the finished plate 1 with the appropriate equipment, it is possible to form it together with the diamond element as one part, which simplifies the manufacturing process of the element being developed due to the absence of gluing, welding or soldering operations.

This principle of constructing the construction of destructive elements fully corresponds to the majority of destructive elements for the development of soils of increased strength (teeth of excavator buckets, tips of soil disintegrator, cutters of bar tools and other material-handling machines).

3.3 Investigation of changes in the operating parameters of two-mass resonant vibrating machines for compaction of construction media

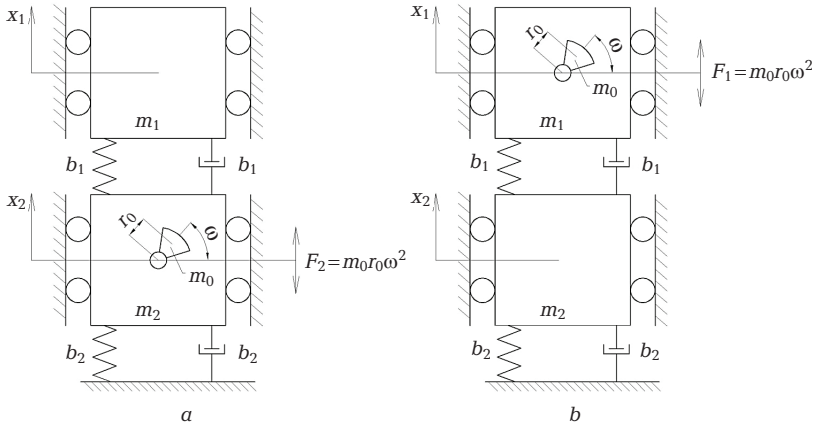
The calculation model of a two-mass resonant vibrating machine for compaction of construction media is represented by two options for the centrifugal arrangement: on the reactive mass (Fig. 3.8, *a*) and on the active mass (working body) (Fig. 3.8, *b*).

Assuming that the resistances are proportional to speed, the differential equations of motion for the first variant of the circuit (Fig. 3.8, *a*) can be written as follows:

$$m_1\ddot{x}_1 + b_1(\dot{x}_1 - \dot{x}_2) + c_1(x_1 + x_2) = F_a e^{i\omega t}; \quad (3.22)$$

$$m_2\ddot{x}_2 - b_1(\dot{x}_1 - \dot{x}_2) - c_1(x_1 - x_2) + b_2\dot{x}_2 + e_2x_2 = 0, \quad (3.23)$$

where F_a – centrifugal force ($F_a = m_0 r \omega^2$).


Fig. 3.8 Design schemes:

- a* – with the installation of a vibration exciter on a reactive mass m_1 ;
b – with the installation of the vibration exciter on the working body m_2

In the last expression m_0 – mass of unbalances, r – eccentricity of the unbalance; ω – angular speed of unbalance rotation.

Denoting:

$$x_1 = \frac{m_0 r \omega^2}{m_2 \omega_0^2} \xi x_2 = \frac{m_0 r \omega^2}{m_2 \omega_0^2} \xi_{12}, \quad (3.24)$$

and after transformations similar to the previous ones, let's obtain:

$$\chi \gamma^2 \xi_1'' + \frac{\chi}{1+\chi} \gamma \beta_1 (\xi_1' - \xi_{12}') + \frac{\chi}{1+\chi} (\xi_{11} - \xi_{12}) = e^{i\tau}; \quad (3.25)$$

$$\gamma^2 \xi_{12}'' = \frac{\chi}{1+\chi} \gamma \beta_1 (\xi_1' - \xi_{12}') + \gamma \beta_2 \xi_{12}' - \frac{\chi}{1+\chi} (\xi_{11} - \xi_{12}) + \gamma^2 \beta_2 \xi_{12} = 0. \quad (3.26)$$

The solution of equations (3.25) and (3.26) gives the value of the dimensionless amplitude of the mass displacements m_1 :

$$\xi_{11a} = \frac{m_2 X_{11a}}{m_0 r} = \gamma^2 \sqrt{\frac{K^2 + M^2}{Z^2 + Y^2}}; \quad (3.27)$$

dimensionless amplitude of mass displacements m_2 :

$$\xi_{12a} = \frac{m_2 X_{12a}}{m_0 r} = \frac{x}{1+x} \gamma^2 \sqrt{\frac{\gamma^2 \beta_1^2 + 1}{Z^2 + Y^2}}; \quad (3.28)$$

dimensionless relative amplitude of mass displacements m_1 and m_2 :

$$\xi_{I_a} = \frac{m_2 X_{I_a}}{m_0 r} = \sqrt{\frac{\left(\frac{x}{1+x} - k\right)^2 + \left(\frac{x}{1+x} \gamma \beta_1 - M\right)^2}{Z^2 - Y^2}}; \quad (3.29)$$

phase angle between displacement and force:

$$\varphi_1 = \text{arctg} \frac{MZ - KY}{KZ + MY}. \quad (3.30)$$

Hereinafter, Roman numerals I and II in the index indicate the corresponding parameters of the machines with the first and second options for installing a centrifugal occasion. The phase shift angle between ξ_{I_2} and the force F :

$$\varphi_2 = \text{arctg} \frac{Z \gamma \beta_1 - Y}{Z + Y \gamma \beta_1}. \quad (3.31)$$

The phase shift angle between ξ_I and the force F :

$$\psi = \text{arctg} \frac{MZ - KY + \frac{\chi}{1+\chi} Z \gamma \beta_1}{KZ + MY - \frac{\chi}{1+\chi} Y \gamma \beta_1}; \quad (3.32)$$

dimensionless power necessary to maintain oscillation:

$$P_{os} = \frac{P m_2}{m_0 r^2 \omega_0^2} = \frac{\gamma^3}{2} \left(\frac{\chi}{1+\chi} \beta_1 \xi_{I_a}^2 + \beta_2 \xi_{I_a}^2 \right). \quad (3.33)$$

The power spent on overcoming friction in bearings about the case can be written as follows:

$$P_{fr} = \frac{F_a f d_s \omega}{2},$$

where d_s – diameter of the shaft under the bearing; f – reduced to the shaft coefficient of friction in the bearing.

Accordingly, in dimensionless expression, the power spent on overcoming friction will be:

$$p = \frac{P_{fr} m_2}{m_0^2 r^2 \omega^3} = \frac{\gamma^3 \Delta_y f}{2\chi}. \quad (3.34)$$

Then the power of the drive motor is:

$$P_m = \frac{(P + P_{fr})m_2}{m_0^2 r^2 \omega_0^2} = \frac{\gamma^2}{2} \left(\frac{\chi}{1+\chi} \beta_1 \xi_{I_a}^2 + \beta_2 \xi_{I_{2a}}^2 \right) + \frac{\gamma^3 \Delta_y f}{2\chi_0}. \quad (3.35)$$

The total moment of resistance arising during the operation of the machine can be expressed as:

$$\Psi_1 = \frac{(M + M_{fr})m_2}{m_0^2 r^2 \omega_0^2} = \frac{\gamma}{2} \left(\frac{\chi}{1+\chi} \beta_1 \xi_{I_a}^2 + \beta_2 \xi_{I_{2a}}^2 \right) + \frac{\gamma^2 \Delta_y f}{2\chi}; \quad (3.36)$$

$$P_{ml} = \frac{(P + P_{fr})m_2}{m_0^2 r^2 \omega_0^2} = \frac{\gamma^2}{2} \left(\frac{\chi}{1+\chi} \beta_1 \xi_{I_a}^2 + \beta_2 \xi_{I_{2a}}^2 \right) + \frac{\gamma^3 \Delta_y f}{2\chi_0}. \quad (3.37)$$

The total moment of resistance arising during the operation of the machine can be expressed as:

$$\Psi_1 = \frac{(M + M_{fr})m_2}{m_0^2 r^2 \omega_0^2} = \frac{\gamma}{2} \left(\frac{x}{1+x} \beta_1 \xi_{I_a}^2 + \beta_2 \xi_{I_{2a}}^2 \right) + \frac{\gamma^2 \Delta_y f}{2x}. \quad (3.38)$$

In the expressions (3.27) – (3.33):

$$K = \gamma^2 - \gamma^2 + \frac{x}{1+x}; \quad (3.39)$$

$$M = \gamma \beta_2^2 + \frac{x}{1+x} \gamma \beta_1. \quad (3.40)$$

Characteristics of machines with a centrifugal drive, made according to the first version of the scheme (Fig. 3.8, *a*) are presented in Fig. 3.9 at $x=0.125$, $\beta_1=0.02$ and $\beta_2=0.15$. The characteristics are constructed from expressions (3.27), (3.28), (3.30), (3.31) and (3.36).

For the second installation option of a centrifugal drive (Fig. 3.8, *b*), the dynamics equation in dimensionless expression will look like:

$$x\gamma^2 \xi_{II1}'' + \frac{x}{1+x} \gamma \beta_1 (\xi'_{II} - \xi_{II2}) + \frac{x}{1+x} (\xi_{II1} - \xi_{II2}) = 0; \quad (3.41)$$

$$\gamma^2 \xi_{II1}'' + \frac{x}{1+x} \gamma \beta_1 (\xi'_{II1} - \xi'_{II2}) + \gamma \beta_2 \xi'_{II} - \frac{x}{1+x} (\xi_{II1} - \xi_{II2}) + \gamma^2 \xi_{II2} = -e^{i\tau}. \quad (3.42)$$

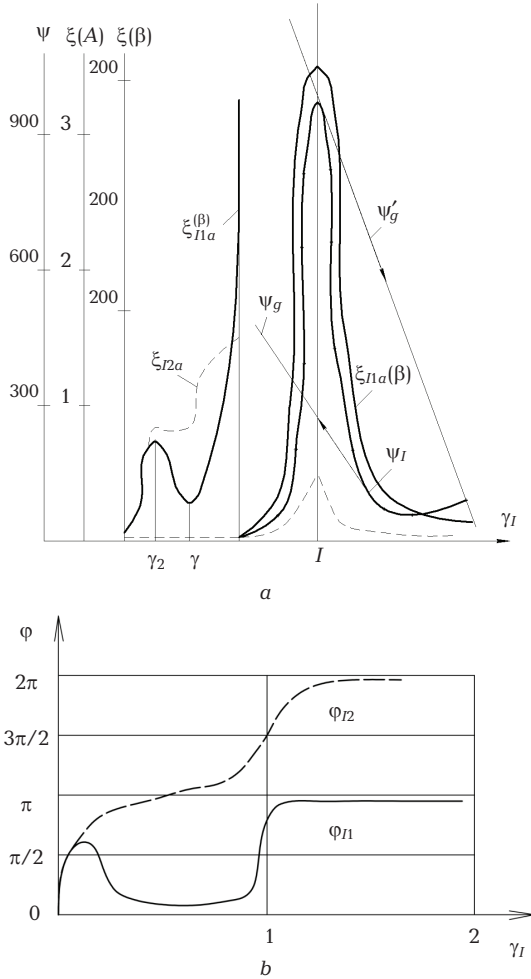


Fig. 3.9 Amplitude (a) and phase-frequency characteristics and static characteristics (b) of the machine and engine for the circuit (Fig. 3.8, a): $x=0.125$; $\beta_1=0.02$; $\beta_2=0.15$

The solution of equations (3.41) and (3.42) gives, for the second option, the dimensionless amplitude of mass m_1 displacement, respectively:

$$\xi_{II_{2a}} = \frac{m_2 x_{II_{1a}}}{m_0 r} = \frac{x}{1+x} \gamma^2 \sqrt{\frac{\gamma^2 \beta_1^2 + 1}{Z^2 + Y^2}}. \quad (3.43)$$

The dimensionless amplitude of mass m_2 displacements:

$$\xi_{II_{2a}} = \frac{m_2 X_{II_{2a}}}{m_0 r} = \gamma^2 \sqrt{\frac{\left(\frac{x}{1+x}\right)^2 \gamma^2 \beta_1^2 + R^2}{Z^2 + Y^2}}. \quad (3.44)$$

The dimensionless amplitude relative to the movement of masses m_1 and m_2 :

$$\xi_{II_a} = \frac{m_2 X_{II_a}}{m_0 r} = \gamma^2 \sqrt{\frac{x}{1+x} + R}. \quad (3.45)$$

Phase shift between ξ_{II_1} and force F :

$$\varphi_1 = \text{arctg} \frac{Z \gamma \beta_1 - Y}{Z + Y \gamma \beta_1}. \quad (3.46)$$

Phase shift between ξ_{II_2} and force F :

$$\varphi_2 = \text{arctg} - \left(\frac{RY + \frac{x}{1+x} Z \gamma \beta_1}{RZ - \frac{x}{1+x} Y \gamma \beta_1} \right). \quad (3.47)$$

Phase shift between ξ_{II} and force F :

$$\psi = \text{arctg}(-Y/Z). \quad (3.48)$$

Power necessary to maintain vibrations:

$$\theta = \frac{N m_2}{m_0^2 r^2 \omega^3} = \frac{\gamma^2}{2} \left(\frac{\chi}{1+\chi} \beta_1 \xi_{II_a}^2 + \beta_2 \xi_{II_{2a}}^2 \right). \quad (3.49)$$

By analogy with the first option, the power of the drive motor can be expressed as:

$$P_m = \frac{(P_l + P_{fr}) m_2}{m_0^2 r^2 \omega_0^2} = \frac{\gamma^2}{2} \left(\frac{x}{1+x} \beta_1 \xi_{II_a}^2 + \beta_2 \xi_{II_{2a}}^2 \right). \quad (3.50)$$

And the total moment of resistance is like:

$$\Psi_{II} = \frac{(M + M_{fr}) m_2}{m_0 r^2 \omega_0^2} = \frac{\gamma}{2} \left(\frac{x}{1+x} \beta_1 \xi_{II_a} + \beta_2 \xi_{II_{2a}} \right) + \frac{\gamma^2 \Delta_y f}{2x_0}. \quad (3.51)$$

In the expressions (3.43) – (3.49):

$$R = x\gamma^2 - \frac{x}{1+x}. \quad (3.52)$$

The characteristics of a centrifugal driven machine, which are made according to the second version of the circuit, built on expressions (3.43), (3.44), (3.46), (3.47) and (3.51), are presented in Fig. 3.10.

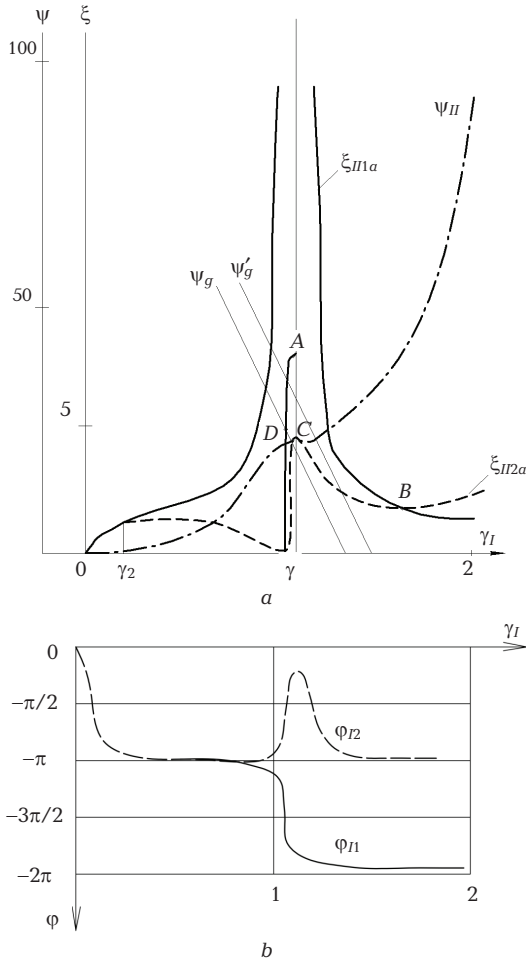


Fig. 3.10 Amplitude and phase-frequency characteristics and static characteristics of a machine and engine for a circuit (Fig. 3.8, b):
 at $x=0.125$; $\beta_1=0.02$; $\beta_2=0.15$

Chapter 4

Experimental investigations of the motion of mechanical systems taking into account the influence of the media

4.1 Experimental investigations of operating modes and parameters of the three-mass vibratory jaw crusher

4.1.1 Experimental device, measuring instruments and research methodology

Experimental studies were carried out on a physical model of a three-mass vibratory jaw crusher, for which proportionality coefficients with a real crusher were determined.

The experimental research program includes the following steps:

- determination of similarity criteria for a physical model and calculation of its parameters;
- development and manufacture of a physical model of a vibratory jaw crusher for conducting experimental studies;
- selection and development of measuring and recording equipment to determine the main operating parameters of the physical model;
- drawing up a plan for the experiment;
- processing of the obtained results, comparison of experimental studies with theoretical ones.

Taking into account the similarity coefficients and based on the objectives of the study, a physical model of the three-mass vibratory jaw crusher was developed, which allows experimental studies. (Fig. 4.1, *a*).

The three-mass vibratory jaw crusher (Fig. 4.1, *a*) consists of three masses that are paired with elastic elements 4 and 9. The first mass of the crusher includes a movable plate 3 to which vibrator 2 is firmly attached (IV-104B6). The second mass includes a prefabricated frame 5 to which the fixed crushing plates 8 are rigidly or pivotally mounted. The crusher frame 5 is supported on the frame 1 through rubber elastic elements 10. The third mass (striker) includes a movable plate 7 to which crushing plates are rigidly attached to

both sides 6. The third mass is mounted in the middle of the crusher frame and rests on special roller bearings 11.

The connection of the vibrator 2 to the power supply is shown in Fig. 4.2, *b*. The contacts of the vibrator 2 are connected in a triangle circuit, as a result of which a potential difference of 220 V occurs at each phase. Next, the vibrator contacts are connected to the frequency converter 13 (DELA VFD-EL) via circuit breakers 14 with a nominal value of 6 A. In turn, the frequency converter 13 is connected to a single-phase power supply network (220 V, 50 Hz), through circuit breakers 12 with a nominal value of 16 A. The frequency converter has an ethernet connector 16, with which it connects to a PC. The vibrator 2 and the frequency converter 13 have a grounding 15.

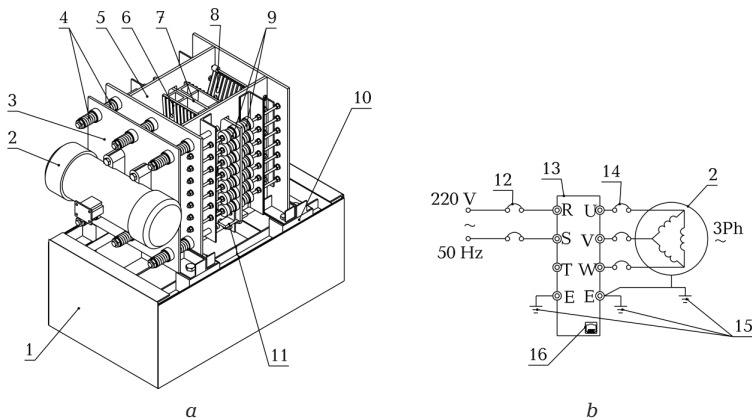


Fig. 4.1 Scheme of the physical model of the three-mass vibratory jaw crusher: *a* – 3D model of three mass vibratory crushers; *b* – control unit

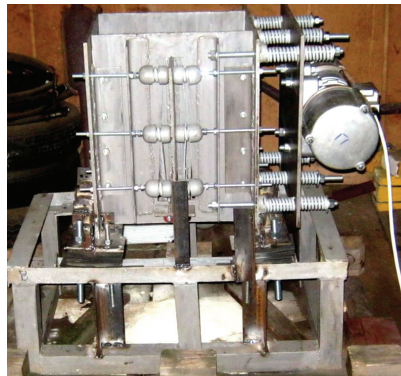


Fig. 4.2 Experimental device of a vibratory crusher

The experimental device in Fig. 4.2 is developed based on the physical model diagram of Fig. 4.1.

The displacements of the structural elements of the crusher are measured using plates with glued strain gauges. To measure the dynamic loads that occur in the material when it is crushed, a pressure sensor was created, which is a wedge. The connection diagram of the sensors for measuring displacements and stresses is shown in the Fig. 4.3. All analog signals are sent to the gain board. After amplification, the analog signal enters the data acquisition system (m-DaQ14), where it is converted into a digital signal and transmitted to a PC. The appearance of the data acquisition system for the vibratory jaw crusher is shown in Fig. 4.4.

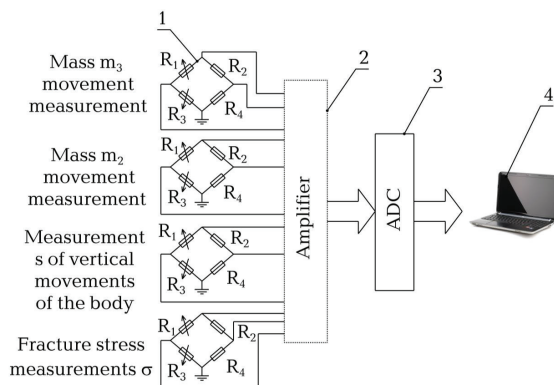


Fig. 4.3 Schematic diagram of a data acquisition system



Fig. 4.4 Appearance of the data acquisition system:

- 1 – experimental device; 2 – control unit; 3 – personal computer, Lenovo G555;
- 4 – ADC, m-DAQ; 5 – gain board based on OP INA125; 6 – measuring sensors

4.1.2 The results of investigations of the influence of design and technological parameters on the crusher efficiency

Vibrograms of oscillations of the third mass of the crusher, provided that there is material in the crushing chamber, are presented in Fig. 4.5 – 4.7. Medium and low strength material was used for crushing.

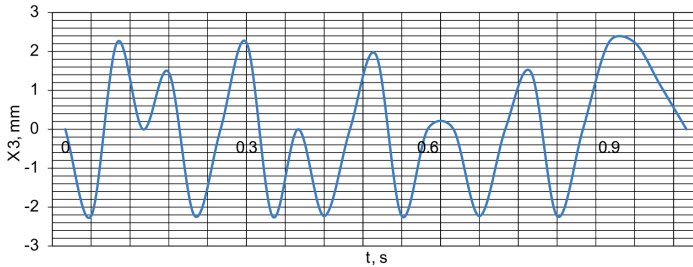


Fig. 4.5 Vibrograms of the third mass of the crusher during its operation with the material ($\omega=75.36$ rad/s, $F=2130$ N, $c_2=219052$ N/m)

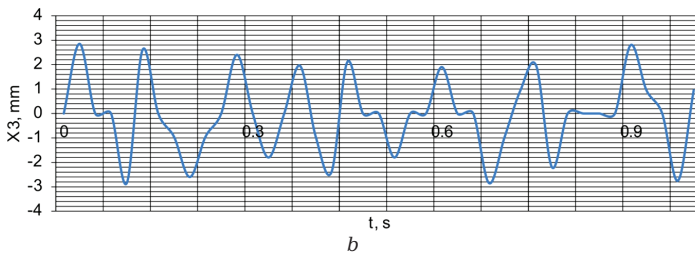
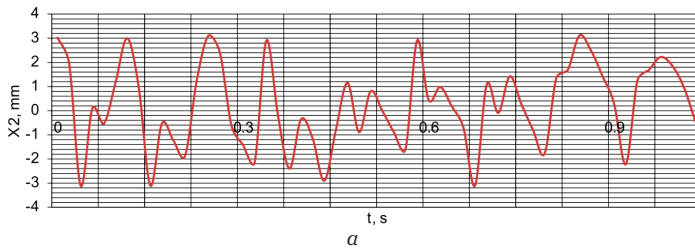


Fig. 4.6 Vibrograms of mass oscillations of the crusher during its operation with material ($\omega=104.667$ rad/s, $F=4111$ N, $c_2=219052$ N/m):
a – movement of the second mass; *b* – movement of the third mass

The range in which experimental studies of the operation of the three-mass vibratory jaw crusher are carried out covers three modes: pre-resonance, near-resonance and out-of-resonance.

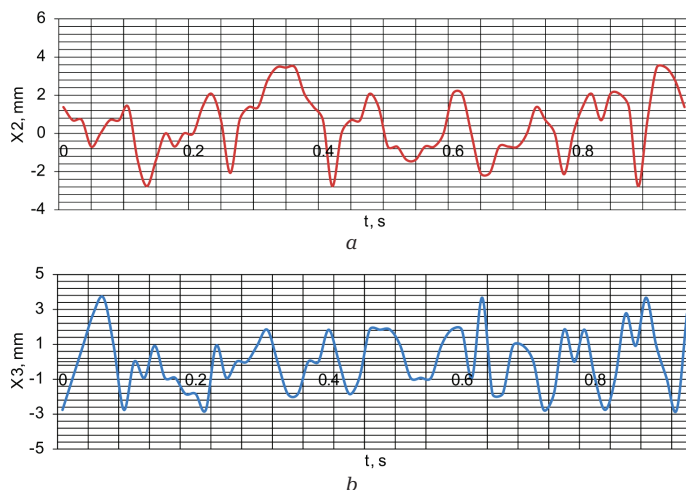


Fig. 4.7 Vibrograms of mass oscillations of the crusher when working with material ($\omega=104.667$ rad/s, $F=4111$ N, $c_2=234438$ N/m):
a – movement of the second mass; *b* – movement of the third mass

When the crusher is operating in the vicinity of a frequency of 12 Hz, almost no material is crushed. This can be explained by the fact that the vibrator does not create efforts at a given frequency that effectively destroy the material. Single destruction can be explained by the presence of significant zones of rupture in the material. To fully characterize this mode, a scheme is suitable in which the striker hits the anvil, the role of the striker in this case is played by the third mass, and the anvil's second mass. Thus, for effective destruction in this range, it is necessary to increase the energy of motion of the third mass. In the frequency range of $14.5 \text{ Hz} < f < 26 \text{ Hz}$, the material is effectively milled. The grinding efficiency is somewhat reduced when the crusher is operating in the vicinity of a frequency of 22 Hz. This can be explained by a decrease in the amplitude of oscillation of the second and third masses and a decrease in vertical vibrations of the crusher body, which increases the residence time of the material in the crushing chamber. From the experiments it follows that the amplitude of the oscillations of the crusher masses between the second and third resonances decreases in the direction of the frequency $f=22$ Hz, and increase with a further increase in frequency. At a frequency in the vicinity of the point $f=15$ Hz, the intrinsic oscillations of the crusher, which are superimposed on high-frequency forced oscillations superimposed by vibrograms of mass oscillations, are also observed visually.

In studying the effect of elasticity of the crusher's elastic systems c_1, c_2 on the crushing process, the following features are established. With an

increase in the elasticity of the system, the effective range of the crusher is shifted toward an increase in the angular frequency. This effect can be seen in the analysis of experimental data, where the amplitudes during crusher operation at a higher elasticity are also greater. This is due to the shift of the resonance point in the direction of increasing the angular frequency of oscillations of the crusher. This property can be used to create a crusher control system. If the elasticities are too low, the efficiency of energy transfer from the vibrator to three masses deteriorates, as evidenced by experimental data. So the amplitudes of the oscillations of the third mass, provided that $c_2 = 140\,663$ N/m, are insignificant. With increasing elasticity c_1 , the range of effective operation of the crusher shifts toward zero. With too much increase in elasticity, the three-mass system turns into a two-mass system. With a decrease in elasticity c_1 , the range of effective operation of the crusher narrows, and in the case of too much decrease in elasticity c_1 , the system leaves the state of equilibrium, which has a negative effect on the crushing process.

4.2 Experimental investigations of changes in the state of dispersed media in the processes of their development by cutting and impact methods

The program for determining the parameters of the destruction of the working media during static and dynamic application of loads provided for experimental studies of the processes of their cutting and impact destruction. The experiments were carried out on the KIBI knocker, which allows to study the processes of destruction of the working medium depending on the required geometric, kinematic and energy parameters of the working medium load.

The KIBI knocker (Fig. 4.8) consists of a guide rod 1, a working load 2, a striker with interchangeable teeth 3 and a centralizer 4.

To determine the cutting parameters at a cutting depth h , a trench widens:

$$B_r = B_c - 2h,$$

where B_c – distance between the cutting edges of the teeth on the striker.

The energy parameters of the process of loading the working medium are determined by the height H of the discharge of the working load. Impacts of the working load on the striker with teeth are carried out in the deepening of the striker to a depth L . During tests, the number n of discharges of the working load and the length of the cutting path L are fixed.

The location on the striker of two symmetrically set teeth allows to compensate for the action of the normal components of the cutting

resistance force and practically eliminate the influence of friction forces along the guide rod.

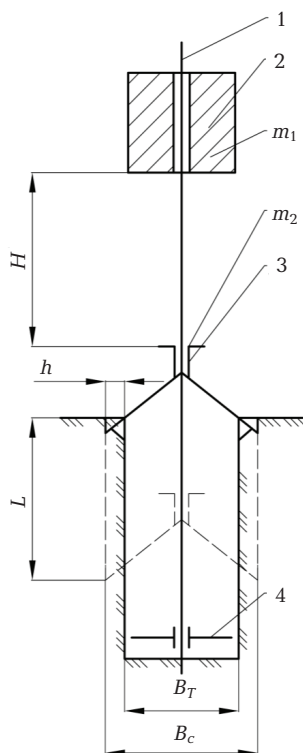


Fig. 4.8 Design diagram of the KIBI knocker:

- 1 – guide rod; 2 – working load; 3 – striker with replaceable teeth;
- 4 – centralizer

Thus, the workflow of the KIBI knocker consists of two phases: 1 – the impact itself (when the impact is very small, which tends to zero and the system moves during the impact are unreasonably small) B_p – cutting of the working medium with a variable speed decreases a certain value to zero (cutting time, cutting path in one stroke).

The average cutting force for each tooth is determined by the formula:

$$P_c = \frac{En}{2L},$$

where E – energy of a single cutting blow.

The energy of a single cutting blow is determined taking into account the decrease in the kinetic energy of the bodies as a result of the impact:

$$-\Delta E = \frac{m_1 \cdot m_2}{2(m_1 + m_2)} (V_1 - V_2)^2 (1 - K^2).$$

This part of the mechanical energy of the system is converted into its internal energy. Here m_1 and m_2 are the mass of the working load and the hammer with teeth; V_1 and V_2 are the speeds of these bodies at the beginning of the impact; K is the recovery coefficient. Given that $V_1 = \sqrt{2qH}$; $V_2 = 0$; $E_1 = m V_1^2 / 2$ and $K=0$ (the impact is absolutely inelastic), the energy of a single cutting blow with the cutting path S , is determined by the formula:

$$E = \frac{m_1^2 q H}{m_1 + m_2}.$$

The cutting process with speeds $V > 1$ m/s is high-speed (dynamic) and has a number of significant differences from quasistatic cutting, in particular, with an increase in the load application speed the ultimate strength and the elastic modulus of the working medium increase, but the ultimate relative deformation and the volume of plastic deformations are significantly reduced, and fracture becomes brittle.

Investigation of the dependence of the cutting force (tangent component) on the energy of a single impact E and the speed V of the hammer with teeth after impact on $K=0$ (the striker with teeth and the working load after impact move as a unit with speed V) is carried out at the stand with a set of working loads weighing from 1 kg to 30 kg with a constant mass of the striker with teeth of 2 kg.

$$V = \frac{m_1 V_1 + m_2 V_2}{m_1 + m_2} \text{ at } V=0;$$

$$V = \frac{m_1 V_1}{m_1 + m_2}.$$

The height H of the discharge of the working load with the mass m_1 providing the necessary speed V and, accordingly, the calculated value E is determined by the formula:

$$H = \frac{1}{2q} \left(\frac{V(m_1 + m_2)}{m_2} \right)^2.$$

The stand has a device for direct recording of the path of the striker with teeth as a function of time t in the process of cutting the working

medium. Schematic diagram of the device for record $S=f(t)$ and an example of record are shown in Fig. 4.9. The nature of the curve $S=f(t)$ indicates that the intensity of the decrease in cutting speed is maximum at the beginning of cutting and comes at the end of the impact, that is, the function $S=f(t)$ has an rapidly decreasing character. When determining the impact on the cutting force of the impact energy E and the initial total cutting speed V , one of these parameters is varied, and all other parameters, such as depth, width and angle of cutting, remain constant.

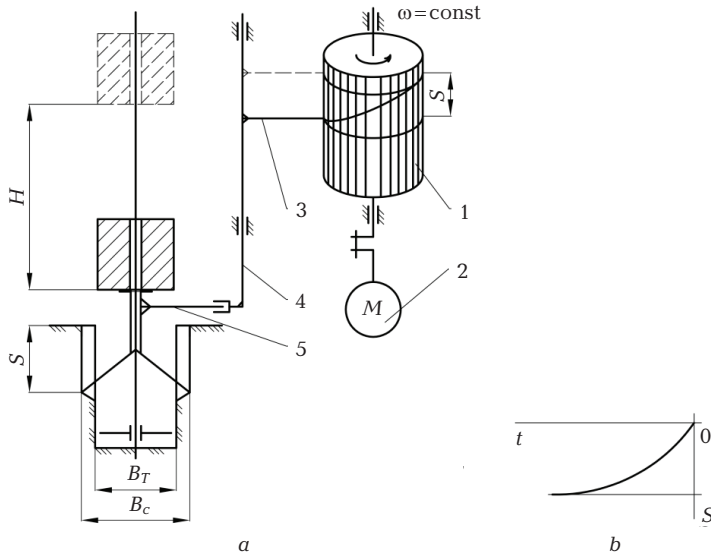


Fig. 4.9 Scheme of the device stand for recording the striker movement with teeth upon impact: *a* – scheme of the device, *b* – example of recording the dependence $S(t)$: 1 – high-speed drum with wax paper; 2 – AC electric motor; 3 – needle; 4 – rod in the guides; 5 – bracket is rigidly fixed to the striker with teeth

An experimental plot of the dependence $P_c = f(E)$ at the same initial speed $V=2$ m/s is shown in Fig. 4.10. The graph shows that, within the parameters, the energy of a single impact E does not affect the cutting force P_c .

The effect of the speed V of the striker with teeth on the force P_c is studied at constant cutting parameters and the energy of a single impact E equal to 10 J. By varying the mass of the working load m_1 in the range from 1 to 30 kg s, the initial total speed and height of the working load N are calculated. Analysis of the results of these experiments (Fig. 4.11) shows that at a constant energy of a single impact E , the cutting force P_c does not depend on the speed V , which varies from 0.8 to 2.2 m/s.

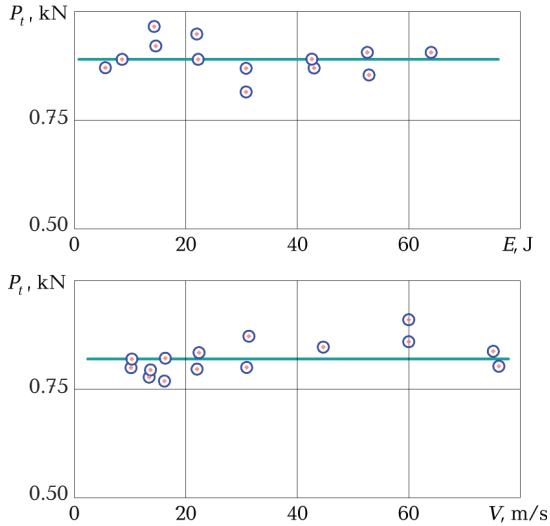


Fig. 4.10 Experimental graphs of the dependence of the average tangential cutting force on the parameters of the shock load

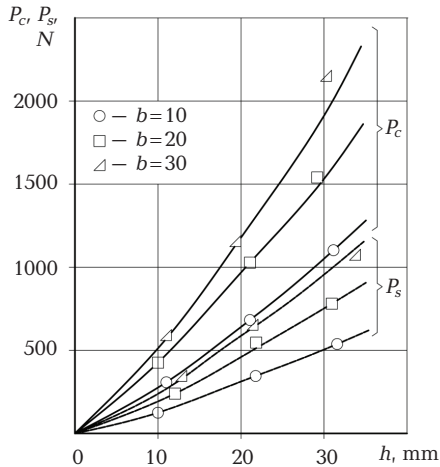


Fig. 4.11 Comparison of the resistance forces of quasistatic and dynamic (impact) cutting versus cut thickness at a constant cutting angle $\delta=45^\circ$

An analysis of the research dependences of the tangential component of the cutting force on the depth h , width b and angle of cutting δ , as well as a comparison of the chip formation parameters, shows that for all media studied (thawed and frozen soils, paraffin, sea ice and frozen ice) they do

not qualitatively differ from similar dependences of the cutting force by quasistatic cutting.

A quantitative comparison of the forces of high-speed (dynamic) and quasistatic cutting was carried out on the basis of the results of experiments on cutting the same paraffin blocks under laboratory conditions with the same cut sizes and cutting angles (Fig. 4.11).

The experiments are carried out by the KIBI knocker and on a dynamic bench with fixation of the tangential cutting force on the oscilloscope. In the experiments at the bench, the cutting tool (teeth) of the KIBI knocker is used, the cutting speed is 0.05 m/s. The average force of quasistatic cutting is determined by the method of planimetric oscillograms.

An analysis of the results shows that, with the same cutting parameters, regardless of the experimental conditions, the cutting force of the KIBI knocker is two times greater than the average tangential cutting force on the dynamometer.

The dependences of the cutting force at various values of the surfaces of interaction of the cutting elements with the working medium show that in high-speed (impact) cutting of working media this process is more efficient, in which most of the energy of high-speed cutting (impact) is concentrated in the area of the cutting edge, which indicates the optimal distribution of flows energy.

4.3 Formation of working processes of soil-grinding machines taking into account the action of physical fields, self-organization and evolution of geometric shapes

Workflows of soil-grinding equipment in an integrated and systematic approach are studied as systems consisting of such significant elements of the subsystem of the complex as a working medium, soil-grinding equipment, the actual processes of interaction of soil-grinding equipment with the working medium and external influences. In addition, the synergistic nature of the interaction between the component subsystems is inherent in this system.

Further development of the soil-grinding equipment and its working processes involves the application of the mechatronic principle for the development of designs of soil-grinding machines and the formation of their working processes. The mechatronic principle is the synergistic combination of precision mechanics with electronic, electrical and computer components and software for controlling the functional movements of machines.

A feature of the development of mechanical components of mechatronic systems is the requirement of maximum reduction in the size of equipment, the compactness of its layout and the consideration of self-organization of geometric shapes of constituent structures.

A significant reduction in the size of the soil-grinding equipment can be achieved due to the redistribution of energy flows (establishment of an individual engine directly on the working body) and the orientation of the working body relative to the bottom of the soil. The principles for the formation of soil face are based on the involvement of existing natural physical fields in the process of destruction of working media. It is known that all real material processes in nature as a general result proceeding in the direction of increasing entropy, therefore, the processes of destruction of working media should be in direct direction in the direction of spontaneous occurrence of natural processes, that is, implement the so-called principle of entropy destruction.

These principles are laid down in the disk working body of the trencher of the KNUCEA design, which makes up a disk with cutting and conveying elements that are located on its working surface. The inclination of the disk at a certain angle α in the vertical plane in the direction opposite to the feed rate forms a slaughter in such a way that the soil is above the working body. Due to this, the force of gravity, which is created by the gravitational field of the earth, acts on soil particles and is aimed at separating these particles from the bottom. This leads to a decrease in the required destruction force of the working medium.

In addition, the soil above the working body is constantly under the influence of waves of stresses (deformations) that occur during single cleavage of the soil due to the high cutting speed. An oscillatory-wave stress-strain state is formed in the volume of soil located above the disk, which is a superposition of direct waves arising from the speed action of cutting elements on the soil during a single cleavage, reflected from the surface of the soil mass and inhomogeneities in the soil and refracted waves forming in areas of heterogeneity of the soil. Due to this stress-strain state, fatigue deformations accumulate in the soil body.

The working movement of the cutting and transporting elements consists of the rotation of the working body about its axis and the translational motion of the base machine, as a result of which the soil is destroyed by the cutting elements. At the same time, the strength of the soil is significantly reduced due to the accumulation of fatigue deformations in it, which leads to a decrease in the energy intensity of cutting. An additional decrease in the energy intensity of soil development is due to the fact that the attractive force helps to separate the soil particles from the soil body. Separated from the soil body, the soil arbitrarily falls onto the working part of the disk and, due to the rotation of the disk, is transported from the bottom by transporting elements. To change the width of the trench in this working body, it is possible to rotate it in a horizontal plane. The decrease in the energy intensity of the soil development process is also affected by the absence of a drawing prism.

The possibility of developing soil almost to the full diameter of the working body, the absence of buckets, the combination of destruction and transportation functions in one body (lack of soil throwers), as well as

a significant reduction (at times) in the energy consumption of cutting leads to a significant reduction in the size and weight of the working body that meets the requirements for mechanical components of mechatronic systems.

During the destruction process, the cutting tools are subject to wear (Fig. 1.11). In this case, a wear site with a negative angle arises, increases the energy consumption of cutting, that is, self-organization and evolution of geometric shapes occur, which must be corrected as in the technical solution (Fig. 1.12).

The wear of the cutting elements is determined by the soil erosion. When studying soil erosion, for example, when loosening it, it is estimated by shortening the tips of the same type under the same conditions with a cutting angle of 45° and a loosening depth of 25...40 cm. Below are given (Table 4.1) the values of relative erosion for the most common soils are developed by soil disintegrators.

Table 4.1 Relative soil erosion

Soil	K_{er}
Frozen light brown loam with inclusions of rock pieces up to 0.05 m in size	1.00
Frozen light brown loam with gravel inclusions	1.05
Frozen sandy loam with inclusions of rocky strata	1.07
Permafrost sandy soil at a temperature of -6°C and humidity of 26 %	1.42
Frozen dark brown loam with separate sections (up to 40 % by area) of monolithic rock	1.90
Homogeneous fractured rock	2.05

Soil erosion increases with an increase in the content of sand particles and solids in them. Coefficients of relative erosion of soils K_{er} presented in Table 4.1 can be used for an approximate calculation of the wear of the tips.

4.4 Experimental investigations of forming design at dynamic load

The object of research is the movement process of forming structures of a vibration unit with spatial oscillations. The main disadvantage of such vibration systems is the lack of data on the mutual influence of machines and media.

The vibration unit simultaneously performs the function of a mold for a concrete mix and consists of a welded box-section frame, which is installed on rubber elastic supports on a concrete foundation. Vibration unit is equipped with two, not symmetrical installed centrifugal generators of high-frequency oscillations. Two non-removable sides and one movable side are fixed on the frame. A geometric 3D model is created to study the vibration unit, on the basis of which the design finite element model is developed (Fig. 4.12).

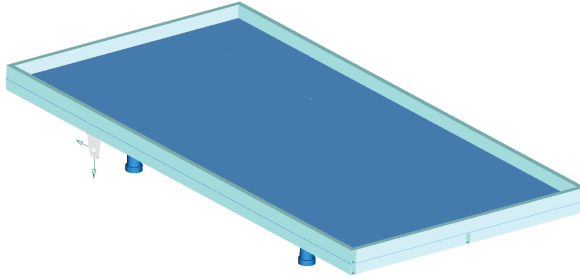


Fig. 4.12 Design 3D model of vibration unit for the formation and compaction of concrete mixtures

The preliminary calculations are performed to determine simple and more complex waveforms. The choice is the possibility of implementing modes of operation with higher levels of energy transfer to the processed medium.

The most interesting issue in the study of such structures is the determination of the laws of energy transfer from the forming surfaces to the processed medium. As well as the use of wave phenomena in the forming surfaces in the implementation of operating modes at the main oscillation frequencies.

The aim of research is experimentally determination of the amplitudes of oscillation forming the surface of the structure of the vibration unit.

To achieve this aim, the following objectives are defined:

1. To develop an experimental model of vibration unit with active forming surfaces.
2. To evaluate the basic frequencies and amplitudes of oscillation of forming surfaces.
3. To test the hypothesis of the presence of wave phenomena in the forming surfaces of the structure of the vibration unit.

A number of works are devoted to the study of vibration units. Thus, in [15], an approach for modeling dynamic systems with distributed parameters is proposed. The given method of taking into account not only elastic, but also dissipative properties of the medium processed during oscillation. In [16], an analytical method is proposed for determining the influence of the processed medium on the dynamics of the «machine – medium» system. The analytical dependences for estimating the influence of the medium resistance at poly-frequency oscillations are obtained. In [17], studies of a shock vibration machine for molding concrete products are given. Studies are based on the determination of the reduced mass and the equivalent coefficient of resistance of a concrete mix. As a result, the dependences for the description of wave phenomena in the medium are obtained. However, the results of experimental determination of the dynamic parameters of the investigated units in the above works are absent. The authors of [18] consider a dynamic system capable of accumulating internal energy. Phenomena in

complex nonlinear systems, as the authors note, are promising direction and require additional research. Experimental studies of the oscillatory system using measurements of accelerations are given in [19]. The study is based on a certain oscillation spectrum and the identification of natural oscillation frequencies. The method can be used to study more complex dynamic systems. Measurements of the dynamic characteristics of systems in order to identify defects in structural elements of applying experimental studies of vibration and their processing are presented. It is proposed to improve the computational model based on the obtained dynamic characteristics. Such an approach can be used to verify the conformity of the mathematical and experimental models of the investigated complex dynamic systems. In [20], the method is applied to nonlinear active vibration control systems. As the authors note, the advantage of such an integral method is that there is no need to know the system parameters, such as mass, attenuation and stiffness coefficients, which are usually obtained by finite element methods. Of course, such data acquisition systems are highly accurate and sensitive. But their application is limited to high cost.

Thus, the results of literary analysis allow to conclude that acceleration measurement sensors are used to measure dynamic parameters. The use of strain gauge measurement methods is one of the modern and effective for fixing dynamic parameters. This is due to the ability to simultaneously record both numerical and qualitative characteristics, taking into account the phase shift.

To implement the research of vibration unit, the following sequence of research works is assumed:

- analysis of calculations of the structural elements of the machine in terms of accounting for all types of loads that are carried out in the machine design;
- development of a computer model of the object of research (general or some of the most loaded nodes, structural elements);
- carrying out additional modeling and calculations to determine the behavior of structural elements and the machine as a whole, while the various loads act simultaneously;
- development on a computer model of a matrix of control points of limiting values of integral characteristics of the structure state for further use in field tests;
- carrying out field tests by applying certain loads on its model;
- adjustments of the computer model until the comparison of the integral characteristics obtained by measuring at the control points during the experiment and in the simulation will differ among themselves within the limits of the permissible error. The computer model obtained in this way will be adequate to the real construction within the limits of adequacy – the points of the integral characteristics control.

In the case of modernization of the existing machine model for technological purposes, the computational model in such a complex will allow

analyzing the technical level of the structure and predicting its reliability. And in combination with the performed experimental studies, assess the current technical condition, the appearance of possible failures, and the like.

On the basis of such studies, it is possible to assess the nature and magnitude of the change in the stress-strain state of elements and steel structures as a whole. This will make it possible to determine the quality of the fabrication of the structure and its compliance with the design data (performance of welds, bolted joints, structural integrity).

The experimental model of the vibration unit is developed on the basis of studies of the computational model [21]. Vibration experimental unit is made of metal. The design consists of a welded tubular frame with forming surfaces. The frame rests on rubber elastic supports. A general view of the vibration unit is shown in Fig. 4.13.

The vibration unit is equipped with two asymmetrically mounted vibration exciters (Fig. 4.14), which are attached to the frame with fasteners. To control the excitation frequency and the unbalance position in space, the vibration exciters are equipped with unbalance position sensors.



Fig. 4.13 General view of the vibration unit



Fig. 4.14 The vibration exciter with unbalance position sensor

To determine the amplitude of oscillations, inductive type displacement sensors are used (Fig. 4.15, *a*). The condition of the forming surfaces is monitored using strain sensors (Fig. 4.15, *b*).

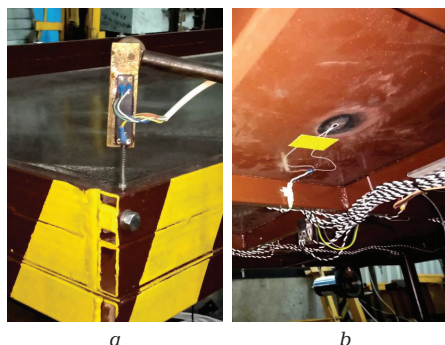


Fig. 4.15 Sensor: *a* – displacements; *b* – deformations

The oscillation amplitude of the investigated unit is determined on the basis of measurements of amplitudes at three points located along the structure. The control of the deformed state of the forming surfaces is carried out on the basis of data from 18 strain gauges. The layout of the measurement sensors is shown in Fig. 4.16.

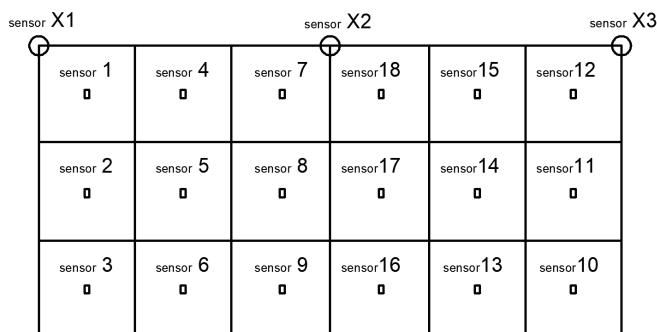


Fig. 4.16 Layout of measurement sensors

Data readings from sensors and their subsequent processing are carried out using the developed circuit based on a 32-bit controller with two independent analog-digital converters. Such a system provides the speed of sampling signals from 20 kHz sensors. Data processing is carried out using a PC. A general view of the experimental unit with the measurement system is shown in Fig. 4.17.

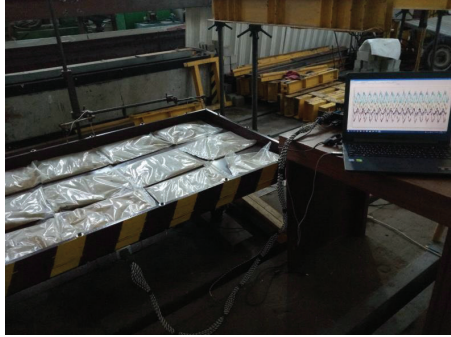


Fig. 4.17 General view of the experimental unit

When conducting experimental studies, a number of oscillograms are obtained on various operating modes of the vibration unit. Typical oscillograms are shown in Fig. 4.18. As can be seen from the oscillogram in Fig. 4.18, there are transients, which are explained by a change in the oscillation frequency.

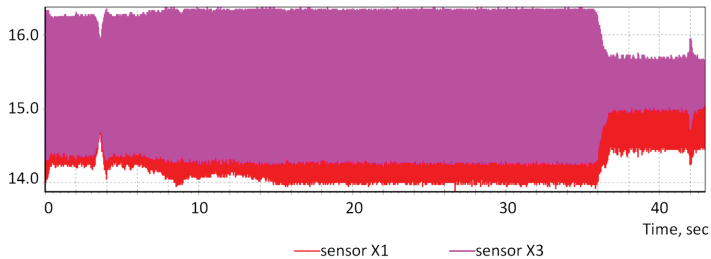


Fig. 4.18 Oscillogram of vibration unit movement

After processing the received oscillograms of vibration unit movements, the main oscillation frequencies are determined. Also, the waveforms that are carried out at these frequencies are analyzed. So, with an excitation frequency of 12.5 Hz, the forming surfaces perform vertical oscillations (Fig. 4.19). The movement of the unit occurs in the common mode, which indicates the realization of the oscillation form, when the whole structure moves progressively in the vertical direction. So, to determine the amplitude of oscillations, sensors of inductive type are used (Fig. 4.16, *a*). The condition of the forming surfaces is monitored using strain sensors (Fig. 4.16, *b*).

The motion of the vibration unit at an excitation frequency of 18.6 Hz and 24.3 Hz, in contrast to the previous one, indicates the realization of an oscillation form with anti-phase movement (Fig. 4.20, 4.21).

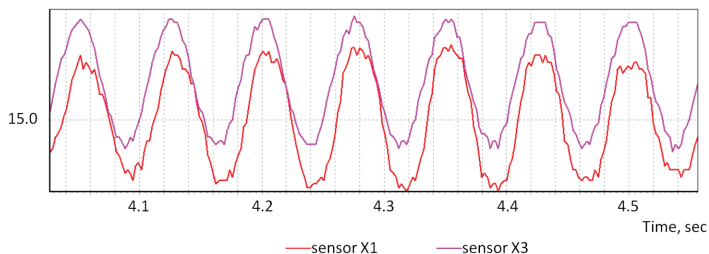


Fig. 4.19 Oscillogram of the vibration unit movement at an oscillation frequency of 12.5 Hz

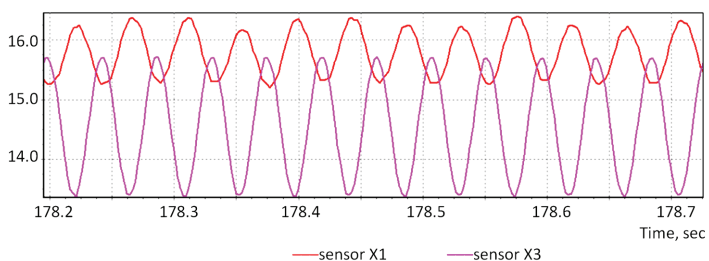


Fig. 4.20 Oscillogram of the vibration unit movement at an oscillation frequency of 18.6 Hz

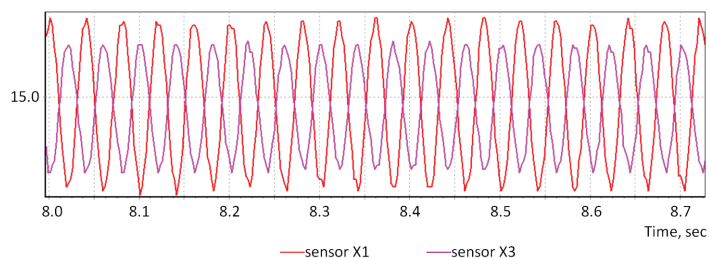


Fig. 4.21 Oscillogram of the vibration unit movement at an oscillation frequency of 24.3 Hz

To assess the stress-strain state of forming structures, the data of strain sensors are analyzed. Based on the obtained results, the following can be noted. When implementing the operating mode at a frequency of 24.3 Hz, a complex stress-strain state arises in the forming surfaces. This is evidenced by various forms and values of deformation in the corresponding parts of the surface. It should also be noted about the presence of wave phenomena (Fig. 4.22, 4.23), which occur in the forming surfaces.

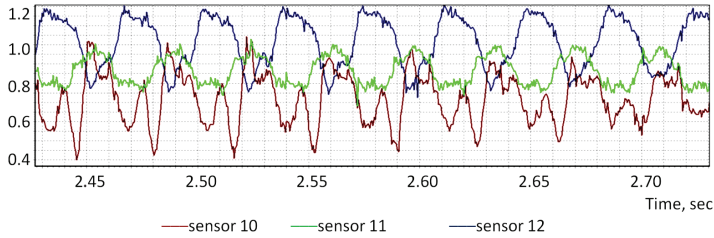


Fig. 4.22 Deformations of the forming surfaces at an oscillation frequency of 24.3 Hz (sensors 10, 11, 12 (Fig. 4.16))

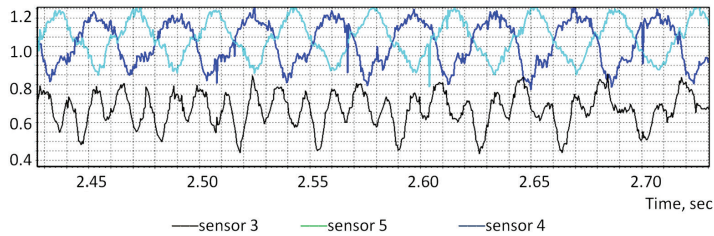


Fig. 4.23 Deformations of the forming surfaces at an oscillation frequency of 24.3 Hz (sensors 3, 4, 5 (Fig. 4.16))

Thus, the presence of poly-frequency (Fig. 4.22, 4.23, sensors 3, 12) and anti-phase character (Fig. 4.23, sensors 4, 5) of oscillograms indicates wave propagation both in the longitudinal and in the transverse directions of the structure.

Research results indicate the presence of complex oscillation forms of forming frame of vibration unit. Thus, the possibility of implementing modes of operation in the presence of wave phenomena in the forming surface is confirmed. This is a proof of research conducted by the authors in [21].

This research has limitations, since unexplored modes of unit operation at higher vibration frequencies. As well as the necessary calculations of qualitative and quantitative indicators of changes in the stress-strain state of the forming surfaces. For objective analysis, several other methods should be applied, such as spectral or wavelet analysis. Such studies are planned by the authors for the future.

A promising direction for further research is the need to search for possible locations of the vibration exciter on the forming surfaces. The second direction of research is the use of parametric oscillations in such systems. In theoretical studies, this solution is effective. The problem is only in the absence of effective constructive and reliable solutions to implement such fluctuations. The possibilities of such research lie in the plane of the development of practical recommendations for the rational constructive design

of sections of forming structures. As well as the development on the basis of certain technological parameters of oscillations of the latest structures similar to the investigated.

The rapid development of the construction industry of Ukraine in the direction of the use of frame-monolithic technology for the construction of constructions and structures displaces machines of this type from the market. But foreign experience shows that there is no need for such machines. The threat may be the lack of machines of this class on the Ukrainian market and the loss of production capacity, which can be applied to the object of research.

Among the threats to this area of research is the attempt of technologists to use auxiliary additives to reduce the need to use vibration methods. At the same time, additional studies of the life cycle of the structures created using this technology are required. Abroad there are similar solutions for other media.

Conclusions

1. To develop technical systems with dynamic effects on processing media, a new approach and methodology is proposed, taking into account the influence of energy fields of physical and mechanical effects, the transformation and inversion of types of energy exposure.

2. A model of considering the structural nature as dispersed media in a wide range of all components of the process of destruction, grinding and compaction is substantiated. The revealed changes in the parameters of the subsystems taking into account their stress-strain state.

3. The parameters of dispersed media as a system of soil destruction, the grinding process, the process of compaction of the processing media in the vibration field are investigated, quantitative and qualitative changes of all significant characteristics of the systems are found.

4. The obtained laws of changing the state of dispersed media under the influence of power loads by technical systems during the implementation of various technological processes have allowed to propose new load processes, including multi-mode implementation with minimized energy costs and increased efficiency of work processes.

5. On the basis of preliminary calculations and modeling of frame bearing elements by beam finite elements, elastically deformed under the action of longitudinal force, bending moments in two planes and torque, an experimental model of vibration unit with active forming surfaces is developed. In the investigation of the system, principles are applied that ensured the model adequacy, as well as the possibility of further research — solving other types of problems.

6. The main oscillation frequencies are determined, which are realized at 12.50 Hz, 18.60 Hz and 24.30 Hz. At the same time, oscillation forms with complex movement of forming surfaces are realized.

7. The presence of wave phenomena in the forming surface is experimentally proved when implementing modes of operation at the main frequencies of oscillations. The amplitudes of oscillations of the unit in the range of 0.0006...0.0003 m are determined at excitation frequencies of 18.60 Hz and 24.30 Hz.

References

1. Nazarenko, I. I. (2007). *Vibratsiini mashyny i protsesy budivelnoi industrii*. Kyiv: KNUBA, 230.
2. Bezruchko, B. N., Korpovskii, A. A. (2005). *Put v sinergetiku. Ekskurs v desiaty lekciakh*. Moscow: Kom. Kniga, 304.
3. Nazarenko, I. I. (2010). *Prykladni zadachi teorii vibratsiinykh system*. Kyiv: Vydavnychi Dim «Slovo», 440.
4. Nazarenko, I. I., Smirnov, V. M., Fomin, A. V. et. al. (2011). *Osnovy teorii vzaiemodii robochykh orhaniv budivelnykh mashyn iz napruzhenodeformovanyam seredovyshchem*. Kyiv: «MP Lesia», 216.
5. Nazarenko, I. I., Harnets, V. M., Sviderskyi, A. T. et. al. (2009). *Systematychnyi analiz tekhnichnykh obektiv*. Kyiv: KNUBA, 164.
6. Loicianskii, L. G. (1973). *Mekhanika zhidkosti i gaza*. Moscow: Nauka, 847.
7. Nazarenko, I. I. (1999). *Mashyny dlia vyrobnytstva budivelnykh materialiv*. Kyiv: KNUBA, 488.
8. Blekhman, I. I., Dzhanelidze, Iu. G. (1964). *Vibracionnoe peremeschenie*. Moscow: Nauka, 368.
9. Babickii, V. I. (1978). *Teoriia vibracionnykh sistem*. Moscow: Nauka, 326.
10. Akhverdov, I. N. (1981). *Osnovy fiziki betona*. Moscow: Stoiizdat, 425.
11. Landau, L. D., Ltvshic, E. M. (1965). *Mekhanika sploshnykh sred*. Moscow: Nauka, 476.
12. Prokhorov, A. M. (1987). *Fizicheskii enciklopedicheskii slovar*. Moscow: Sovetskaia enciklopediia, 944.
13. Mazur, M. P., Vnukov, Yu. M., Dobroskok, V. L., Zaloha, V. O., Novosolov, Yu. K., Yakubov, F. Ya.; Mazur, M. P. (Ed.) (2011). *Osnovy teorii rizannia materialiv*. Lviv: «Novyi Svit – 2000», 422.
14. Fomin, A. V., Kosteniuk, O. O., Teteriatnyk, O. A., Bokovnia, H. I., Zhyhailo, V. V. (2014). Pat. 94978 UA. Rozbrobliuvalnyi element. MPK: B28D 1/04. No. u 2014 06078; declared: 02.06.2014; published: 10.12.2014, Bul. No. 23.
15. Nazarenko, I. I., Sviderski, A. T., Dedov, O. P. (2011). Design of New Structures of Vibro-Shocking Construction Machines by Internal Characteristics of Oscillating System. The Seventh Triennial International Conference HEAVY MACHINERY HM 2011, 2, 1 – 4.
16. Dedov, O. (2018). Determining the influence of the medium on the dynamics of the machine on the basis of spectral analysis. Control,

- Navigation and Communication Systems, 4 (50), 69–72. doi: <http://doi.org/10.26906/sunz.2018.4.069>
17. Nesterenko, M., Nesterenko, T., Skliarenko, T. (2018). Theoretical Studies of Stresses in a Layer of a Light-Concrete Mixture, Which is Compacted on the Shock-Vibration Machine. *International Journal of Engineering & Technology*, 7 (3.2), 419–424. doi: <http://doi.org/10.14419/ijet.v7i3.2.14564>
 18. Andò, B., Baglio, S., Bulsara, A. R., Marletta, V., Pistorio, A. (2015). Experimental and Theoretical Investigation of a Nonlinear Vibrational Energy Harvester. *Procedia Engineering*, 120, 1024–1027. doi: <http://doi.org/10.1016/j.proeng.2015.08.701>
 19. Kavyanpoor, M., Shokrollahi, S. (2019). Dynamic behaviors of a fractional order nonlinear oscillator. *Journal of King Saud University – Science*, 31 (1), 14–20. doi: <http://doi.org/10.1016/j.jksus.2017.03.006>
 20. Jia, Y., Seshia, A. A. (2014). An auto-parametrically excited vibration energy harvester. *Sensors and Actuators A: Physical*, 220, 69–75. doi: <http://doi.org/10.1016/j.sna.2014.09.012>
 21. Nazarenko, I., Gaidaichuk, V., Dedov, O., Diachenko, O. (2017). Investigation of vibration machine movement with a multimode oscillation spectrum. *Eastern-European Journal of Enterprise Technologies*, 6 (1 (90)), 28–36. doi: <http://doi.org/10.15587/1729-4061.2017.118731>